


Unraveling Environmental Forces Shaping Surface Sediment Geochemical “Isodrapes” in the East Asian Marginal Seas

Journal Article

Author(s):

Paradis, Sarah ; Diesing, Markus; Gies, Hannah; Haghipour, Negar; Narman, Lena; Magill, Clayton; Wagner, Thomas; Galy, Valier V.; Hou, Pengfei; Zhao, Meixun; Kim, Jung-Hyun; Shin, Kyung-Hoon; Lin, Baozhi; Liu, Zhifei; Wiesner, Martin G.; Statterger, Karl; Chen, Jianfang; Zhang, Jingjing; Eglinton, Timothy I.

Publication date:

2024-04

Permanent link:

<https://doi.org/10.3929/ethz-b-000668650>

Rights / license:

[Creative Commons Attribution-NonCommercial 4.0 International](#)

Originally published in:

Global Biogeochemical Cycles 38(4), <https://doi.org/10.1029/2023GB007839>

Funding acknowledgement:

184865 - Climate and Anthropogenic PerturbationS of Land-Ocean Carbon trackS (CAPS-LOCK3) (SNF)

215163 - Climate and Anthropogenic PerturbationS of Land-Ocean Carbon TrackS+ (CAPS-LOCK+) (SNF)

Global Biogeochemical Cycles®



RESEARCH ARTICLE

10.1029/2023GB007839

Unraveling Environmental Forces Shaping Surface Sediment Geochemical “*Isodrapes*” in the East Asian Marginal Seas

Key Points:

- The distribution of organic matter in the East Asian marginal seas is governed by its provenance and hydrodynamic processes
- Three distinct *isodrapes* are found, driven by organic matter contents, its age, and mineral surface area
- Spatial machine learning can be an efficient tool to understand the distribution of organic matter in continental margins

Supporting Information:

Supporting Information may be found in the online version of this article.

Correspondence to:

S. Paradis,
sparadis@ethz.ch

Citation:

Paradis, S., Diesing, M., Gies, H., Haghypour, N., Narman, L., Magill, C., et al. (2024). Unraveling environmental forces shaping surface sediment geochemical “*isodrapes*” in the East Asian marginal seas. *Global Biogeochemical Cycles*, 38, e2023GB007839. <https://doi.org/10.1029/2023GB007839>

Received 10 MAY 2023

Accepted 10 MAR 2024

Author Contributions:

Conceptualization: Sarah Paradis, Timothy I. Eglinton












Data curation: Sarah Paradis

Funding acquisition: Thomas Wagner, Valier V. Galy, Meixun Zhao, Jung-Hyun Kim, Kyung-Hoon Shin, Zhifei Liu, Martin G. Wiesner, Karl Stattegger, Timothy I. Eglinton

Investigation: Sarah Paradis, Negar Haghypour, Lena Narman

Methodology: Sarah Paradis, Markus Diesing, Hannah Gies

Resources: Clayton Magill, Thomas Wagner, Valier V. Galy, Pengfei Hou, Meixun Zhao, Jung-Hyun Kim, Kyung-Hoon Shin, Baozhi Lin,

Sarah Paradis¹ , Markus Diesing² , Hannah Gies¹ , Negar Haghypour^{1,3} , Lena Narman⁴, Clayton Magill⁴, Thomas Wagner⁴ , Valier V. Galy⁵, Pengfei Hou⁶, Meixun Zhao^{6,7}, Jung-Hyun Kim⁸ , Kyung-Hoon Shin⁹ , Baozhi Lin¹⁰ , Zhifei Liu¹⁰, Martin G. Wiesner^{11,12}, Karl Stattegger¹³, Jianfang Chen¹² , Jingjing Zhang¹² , and Timothy I. Eglinton¹ 

¹Geological Institute, ETH Zürich, Zürich, Switzerland, ²Geological Survey of Norway, Trondheim, Norway, ³Laboratory of Ion Beam Physics, ETH Zürich, Zürich, Switzerland, ⁴The Lyell Centre, Heriot-Watt University, Edinburgh, UK, ⁵Department of Marine Chemistry and Geochemistry, Woods Hole Oceanographic Institution, Woods Hole, MA, USA, ⁶Frontiers Science Center for Deep Ocean Multispheres and Earth System, Key Laboratory of Marine Chemistry Theory and Technology, Ministry of Education, Ocean University of China, Qingdao, China, ⁷Laoshan Laboratory, Qingdao, China, ⁸Korea Polar Research Institute, Incheon, South Korea, ⁹Department of Marine Sciences and Convergent Technology, Hanyang University ERICA Campus, Ansan-si, South Korea, ¹⁰State Key Laboratory of Marine Geology, Tongji University, Shanghai, China, ¹¹Institute of Geology, University of Hamburg, Hamburg, Germany, ¹²Second Institute of Oceanography, Hangzhou, PR China, ¹³Institute of Geology, Adam Mickiewicz University, Poznań, Poland

Abstract As major sites of carbon burial and remineralization, continental margins are key components of the global carbon cycle. However, heterogeneous sources of organic matter (OM) and depositional environments lead to complex spatial patterns in sedimentary organic carbon (OC) content and composition. To better constrain the processes that control OM cycling, we focus on the East Asian marginal seas as a model system, where we compiled extensive data on the OC content, bulk isotopic composition ($\delta^{13}\text{C}$ and $\Delta^{14}\text{C}$), total nitrogen, and mineral surface area of surficial sediments from previous studies and new measurements. We developed a spatial machine learning modeling framework to predict the spatial distribution of these parameters and identify regions where sediments with similar geochemical signatures drape the seafloor (i.e., “*isodrapes*”). We demonstrate that both provenance (44%–77%) and hydrodynamic processes (22%–53%) govern the fate of OM in this margin. Hydrodynamic processes can either promote the degradation of OM in mobile mud-belts or preserve it in stable mud-deposits. The distinct isotopic composition of OC sources from marine productivity and individual rivers regulates the age and reactivity of OM deposited on the sea-floor. The East Asian marginal seas can be separated into three main *isodrapes*: hydrodynamically energetic shelves with coarser-grained sediment depleted in OC, OM-enriched mud deposits, and a deep basin with fine-grained sediments and aged OC affected by long oxygen exposure times and petrogenic input from rivers. This study confirms that both hydrodynamic processes and provenance should be accounted for to understand the fate of OC in continental margins.

Plain Language Summary This study focuses on carbon cycle processes occurring in marine sediments of the East Asian marginal seas. We compiled extensive data on the organic carbon content and composition of surface sediments in these seas and developed a machine learning model to predict their spatial patterns and identify the environmental conditions that drive their distribution. We found that the spatial distribution of organic matter is governed by the resuspension of different grain size fractions due to water current intensity as well as the contrasting origin of the organic matter (marine, terrestrial, and rock-derived) that influences its reactivity. We also identified three main areas where sediments with similar composition drape the seafloor: shelves with strong bottom current with less organic matter, mud deposits rich in organic matter, and a deep basin with aged organic matter. Understanding the factors that control the distribution of organic matter in these areas is important for accurately assessing their contribution to the global carbon cycle.

© 2024 The Authors.

This is an open access article under the terms of the [Creative Commons Attribution-NonCommercial License](https://creativecommons.org/licenses/by-nc/4.0/), which permits use, distribution and reproduction in any medium, provided the original work is properly cited and is not used for commercial purposes.

1. Introduction

Despite only comprising 15% of the ocean area, continental margins are important sites of organic carbon (OC) storage since they receive organic matter (OM) from both terrestrial and marine sources, and account for the

Zhifei Liu, Martin G. Wiesner,
Karl Statterger, Jianfang Chen,
Jingjing Zhang, Timothy I. Eglinton
Supervision: Timothy I. Eglinton
Validation: Sarah Paradis
Visualization: Sarah Paradis
Writing – original draft: Sarah Paradis
Writing – review & editing:
Sarah Paradis, Markus Diesing,
Hannah Gies, Clayton Magill,
Thomas Wagner, Valier V. Galy,
Meixun Zhao, Martin G. Wiesner,
Timothy I. Eglinton

burial of ~90% of sedimentary OC (Bianchi et al., 2018; Harris et al., 2014; Hedges & Keil, 1995). The preservation of OC in marine sediments is highly dependent on its sources (i.e., recently synthesized biospheric marine or terrestrial OM, or petrogenic carbon from eroded bedrock), which often dictate its reactivity given their contrasting chemical composition: while fresh marine OM is more reactive than terrestrial biogenic organic residues derived from plants and soils, petrogenic OC has the most recalcitrant nature (Bianchi et al., 2018; Blair & Aller, 2012). Hydrodynamic processes also influence the fate of OC since components of OM are preferentially associated with fine-grained sediments with the highest mineral-specific surface area (Keil et al., 1998; Mayer, 1994) that may be prone to resuspension. In addition, this mineral binding can also serve a protective role by limiting the degradation of OC and promoting its aging during sediment redistribution (Ausín et al., 2021; Bao et al., 2016, 2018; Hedges & Keil, 1995; Hemingway et al., 2019). Hence, combined analysis of the spatial distribution not only of OC content, but also characteristics such as its isotopic and elemental composition ($\delta^{13}\text{C}$, $\Delta^{14}\text{C}$, and C/N values) and mineral surface area, which can provide insight of the origin and quality of sedimentary OM, is crucial to understand the underlying processes that modulate the fate of OC in marine sediments (Ausín et al., 2023; Bao et al., 2018; Bröder et al., 2016; Goñi et al., 2013; Gordon & Goñi, 2003; Kim et al., 2022; Vonk et al., 2012).

The East Asian marginal seas comprise one of the largest continental margin systems with a wide variety of depositional environments characterized by semi-enclosed shelves (e.g., Bohai Sea, Yellow Sea, Gulf of Tonkin, Gulf of Thailand), broad continental shelves (e.g., East China Sea, Sunda shelf) as well as a narrow continental shelf (e.g., Vietnamese shelf), and a deep central basin (e.g., central South China Sea). In addition, OC exported by the rivers that discharge into this margin have contrasting isotopic composition and age, leading to the deposition of OM with different quality and degree of degradation. Consequently, contrasting degrees of terrestrial influence, marine productivity and physical processes will affect the content, composition and fate of OC in marine sediments (Figure 1).

Diverse studies in these margins have identified that complex hydrodynamic processes are the dominant factor that affect the distribution of OC, leading to the formation of mud deposits and mobile-muds with contrasting OC origin and remineralization processes (Bao et al., 2018; Hou et al., 2023; Shi et al., 2003; Yao et al., 2014; Zhao et al., 2018; Zhu & Chang, 2000), whereas winnowing of fine-grained sediment enriched in OC promotes its dispersal to deeper distal areas (Kao et al., 2003; Zhu, Wagner, et al., 2011; Zhu, Wang, et al., 2011). These hydrodynamic processes also affect the composition of OC, with the preferential degradation of the most reactive and youngest OC fraction (Bao et al., 2016, 2019), supporting the dispersal of less reactive terrestrial OM to more distal areas (Bai et al., 2021; Fu et al., 2022; Hu et al., 2012; B. Lin et al., 2024; Sun et al., 2021; Wu et al., 2013). Evidence of aging of OC can also be confounded by the contrasting contributions of terrestrial OC from rivers with distinct isotopic compositions. For instance, the Yellow River has considerably more aged OC in comparison to the Pearl River, the Mekong River and the rivers discharging into the Gulf of Thailand (Hou et al., 2020; B. Lin et al., 2023; Tao et al., 2018; Yu et al., 2019), leading to considerably lower $\Delta^{14}\text{C}$ values in the dispersal pathway of the Yellow River in comparison to marine sediments offshore the latter rivers (Bao et al., 2016; B. Lin et al., 2023; Wei et al., 2020; B. Zhao et al., 2021). At the other end of the spectrum, erosive processes of mountainous rivers draining Taiwan lead to the export and dispersal of significant amounts of rock-derived “petrogenic” OC offshore of this island (Kao et al., 2014; B. Lin et al., 2020). Finally, physical protection of OM is highly modulated by its association with mineral surfaces, which can affect its dispersal and preservation in marine sediments (Blattmann et al., 2018, 2019).

These observed contrasting processes demonstrate the complex array of factors that can influence the distribution of OC in surficial marine sediments of the East Asian marginal seas (Bao & Blattmann, 2020). The wealth of studies assessing the distribution of OC, its characteristics and its sources in this area as well as the available data (Tables S1–S7 in Supporting Information S1) provide an exceptional and innovative opportunity to employ spatial machine learning techniques to predict the distribution of sedimentological and geochemical properties of surficial sediments in the East Asian marginal seas. The aim of this novel study is to harness the potential of well-established machine learning methods, which have not yet been fully explored as tools to deconvolve biogeochemical processes occurring on the seafloor, in order to assess the regional-scale processes that affect the fate of OC in a highly complex marginal sea system, and to identify regions where sediment with distinct geochemical composition drape the seafloor. As databases continue to grow and become available, this approach involving the application of classical machine learning algorithms can serve as a guide to understand the fate of OM in other continental margins.

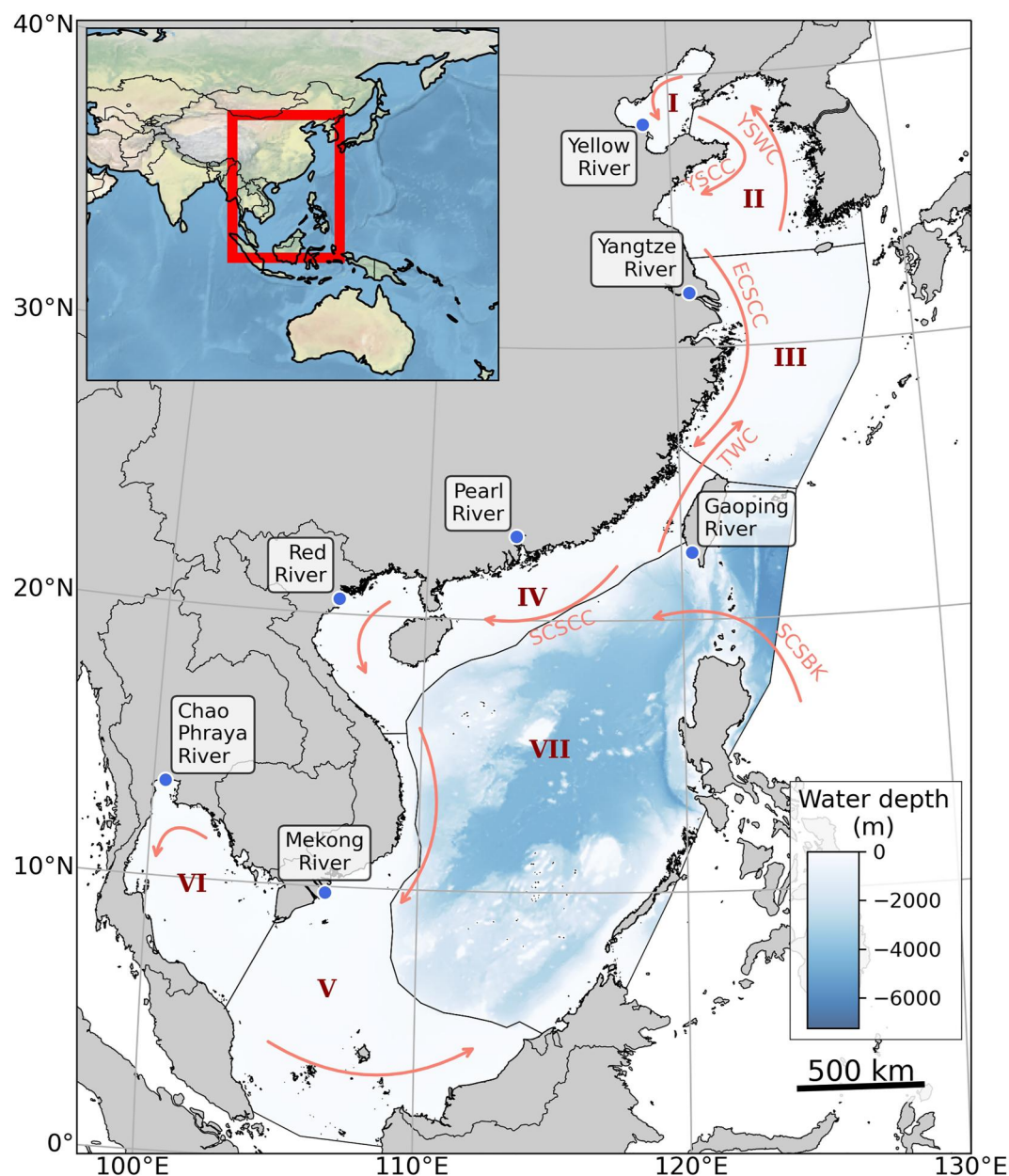


Figure 1. Map of study area, separated into different regions (I-VII). While over 90 rivers discharge into the East Asian marginal seas from the Korean peninsula, China, Taiwan, Vietnam, Thailand, Malaysia, and the Philippines, only the locations of key rivers with the highest sediment discharge are shown. Pink arrows indicate the main current directions of the Yellow Sea Warm Current (YSWC), Yellow Sea Coastal Current (YSCC), East China Sea Coastal Current (ECSCC), Taiwan Warm Current (TWC), South China Sea Coastal Current (SCSCC), South China Sea Branch of Kuroshio (SCSBK), adapted from B. Hu et al. (2014), Z. Liu et al. (2016), and Yao et al. (2015).

2. Study Area

The East Asia marginal seas are comprised by several regions, each with distinct processes. The most influential processes occurring in each region are highlighted below.

Region I in the north is a small enclosed shallow marginal sea that encompasses the Bohai Sea, with a mean water depth of 18 m. Sedimentation rates in this region are highest offshore the Yellow River (Huanghe) (Hu et al., 2011) given its high sediment discharge, with a sediment yield of 150 Mt yr^{-1} (Milliman & Farnsworth, 2011) (Figure 1), and decrease with distance from the river mouth to 0.15 cm yr^{-1} (Wang et al., 2008)

Table 1
Compilation of Clay Mineralogy and Sedimentation Rates in the East Asian Marginal Seas When Available

Region	Illite (%)	Chlorite (%)	Kaolinite (%)	Smectite (%)	References of clay mineralogy	Sedimentation rates (cm-yr ⁻¹)	References
I	48–66	8–24	9–18	1–23	Dou et al. (2014)	0.15–4	L. Hu et al. (2011) and Wang et al. (2008)
II	66–71	12–18	10–14	0–13	Cho et al. (2015) and Park and Khim (1992)	0–1.84	Alexander et al. (1991), Guo et al. (2021), Tao et al. (2016), Yang et al. (2021), Yu et al. (2022), and Zhou et al. (2014)
III	56–79	12–29	0–13	0–12	S. Liu et al. (2014) and Xu et al. (2009)	0–6.3	Chen et al. (2004), DeMaster et al. (1985), Guo et al. (2021); B. Hu et al. (2014), Huh and Chen (1999); Huh & Su (1999), J. P. Liu et al. (2006), and Yang et al. (2021)
IV	29–44	17–27	9–37	10–45	Z. Liu et al. (2010)	–	–
V	23–63	6–27	2–45	0–44	Li et al. (2012) and Szezućiński et al. (2013)	0.2 – > 10	van den Bergh et al. (2007), Szezućiński et al. (2013), and Unverricht et al. (2013)
VI	–	–	–	–	–	0.15–0.78	Srisuksawad et al. (1997)
VII	40–60	3–15	6–27	10–45	Z. Liu et al. (2010)	0.002–0.003	Kuehl et al. (1993)

(Table 1). Weakening of tidal currents in the center of this region promotes the formation of mud deposits enriched in OC (Zhao et al., 2021; Zhu & Chang, 2000).

Region I is connected to Region II through a small strait known as the Bohai Strait. Region II is semi-enclosed by mainland China to the west and the Korean peninsula to the east and it is also relatively shallow, with an average water depth of 44 m, and includes the Yellow Sea (Figure 1). This marginal sea also receives significant amounts of sediment from the Yellow River, which is transported through the Bohai Strait by the Yellow Sea Coastal Current (YSCC) (Figure 1) (Bao et al., 2019; Yang et al., 2011), as well as from sediment eroded from the old Yellow River delta (Zhou et al., 2014), but has lower sedimentation rates than Region I (Table 1). Meso-scale cold cyclonic eddies formed by the Yellow Sea Warm Current (YSWC; Figure 1) lead to mud deposits in the center of Region II where sedimentation rates are highest (1.8 cm yr^{-1}) (Alexander et al., 1991) (Table 1).

Region III includes the East China Sea, a broad continental shelf that extends hundreds of kilometers offshore to the shelf-break (120 m water depth). The Yangtze River (Changjiang) has the highest sediment yield of the rivers discharging in the East Asian marginal seas, which delivered 490 Mt yr^{-1} until the construction of the Three Gorges Dam in 2009, resulting in a reduced sediment yield of 180 Mt yr^{-1} (Z. Yang et al., 2006). Fine-grained sediment discharged by this river is redirected southward by the East China Sea Coastal Current (ECSCC) and, together with the northward flowing Taiwan Warm Current (TWC), promotes the formation of the coastal mobile mudbelt on the inner shelf of the East China Sea (Liu et al., 2007). An additional mudbelt occurs offshore due to the presence of cyclonic eddies (Shi et al., 2003). Sedimentation rates adjacent to the Yangtze River mouth are highest ($>6 \text{ cm yr}^{-1}$), and decrease to negligible values along the highly hydrodynamic shelf that limit the accumulation of sediment (Table 1). The TWC also contributes to the transport of sediment from Taiwanese rivers to Region III (S.-J. Kao et al., 2014; B. Zhao et al., 2021).

Region IV encompasses the Taiwan Strait, the southern Chinese shelf, and the Gulf of Tonkin (Gulf of Beibu). This region is influenced mostly by Taiwanese rivers (e.g., Jhuoshuei River, 40 Mt yr^{-1}), the Pearl River (84.3 Mt yr^{-1}) that discharges in the southern Chinese shelf, and the Red River (130 Mt yr^{-1}) that discharges into the Gulf of Tonkin (S. J. Kao & Milliman, 2008; Z. Liu et al., 2016; Milliman & Farnsworth, 2011). To the best of our knowledge, sedimentation rates have not yet been quantified in this region (Table 1).

Region V includes the narrow Vietnamese Shelf to the north and the broad Sunda shelf offshore the Mekong River in the south (Figure 1); this latter river is the most important in this region, discharging an average of 160 Mt yr^{-1} (Z. Liu et al., 2016). Offshore the Mekong River, sedimentation rates can be greater than 10 cm yr^{-1} , but these rapidly decrease further offshore to 0.2 cm yr^{-1} in the most distal areas (Table 1).

Region VI consists of the Gulf of Thailand, a relatively shallow (70 m) semi-enclosed sea that receives sediment from the numerous rivers that discharge from Vietnam, Cambodia, Thailand, and Malaysia that engulf this region (B. Lin et al., 2023), and the Chao Phraya River in the northern Gulf of Thailand has the largest sediment discharge of these rivers (Z. Liu et al., 2016; Milliman & Farnsworth, 2011; B. Wu et al., 2020) (Figure 1). Sediments from the Mekong River can also reach Region VI advected by the regional cyclonic current (Xue et al., 2014). However, monsoonal winds can reverse the flow to an anticyclonic circulation (J. T. Liu et al., 2016; Z. Liu et al., 2016), which contribute to the formation of mud deposits in the lower area of this region, down-current from the main rivers (Bai et al., 2021; B. Lin et al., 2023; B. Wu et al., 2020). Sedimentation rates offshore the Chao Phraya River and in these mud deposits are highest, ranging between 0.4 and 0.7 cm yr^{-1} whereas lowest sedimentation rates of 0.1 – 0.2 cm yr^{-1} occur in the eastern and central basins (Srisuksawad et al., 1997) (Table 1).

Finally, Region VII encompasses the deep (200–7,000 m) distal basin known as the South China Sea and receives reworked sediment from regions IV and V through the many submarine canyons that incise the continental slopes (L. Lin et al., 2019; Z. Liu et al., 2016) but also from the direct input of Taiwanese rivers such as the Gaoping River that can channel large fluvial sediment through its connected submarine canyon as hyperpycnal flows (Kao et al., 2014; J. T. Liu et al., 2016; Z. Liu et al., 2016). A general cyclonic current occurs in the South China Sea, although it can often be reversed by seasonal monsoons, while several meso-scale eddies are formed by the intrusion of the Kuroshio Current as the South China Sea Branch of Kuroshio (SCSBK) in this basin (Figure 1) (Fang, 1998; J. T. Liu et al., 2016; Z. Liu et al., 2016). Clay mineralogy deposited in Region VII has the highest contribution of smectite (10%–45%) than the remaining regions characterized mostly of illite (~60%) and chlorite (~25%) (Table 1) due to the influence of the several volcanoes present along the Luzon arc system toward the East

of this region (Liu et al., 2010). Some of this smectite can also reach offshore areas of regions IV and V through eolian transport, although its contribution in these regions is minimal (Liu et al., 2010). This deep basin has the lowest sedimentation rates, with relatively constant values that ranged between $0.002 \text{ cm}\cdot\text{yr}^{-1}$ and $0.003 \text{ cm}\cdot\text{yr}^{-1}$ (Table 1).

3. Materials and Methods

3.1. Data Collection and Harmonization

3.1.1. Response Variables

A compilation of data comprising OC and total nitrogen (TN) content, bulk $\delta^{13}\text{C}$ and $\Delta^{14}\text{C}$ values, and mineral-specific surface area for surficial sediment (i.e., within the upper 5 cm to mask seasonal to short-term interannual variations) was extracted from the Modern Ocean Sedimentary Archive and Inventory of Carbon (MOSAIC) database (Paradis et al., 2023; van der Voort et al., 2021) which derived from 60 publications (Tables S1–S7 in Supporting Information S1). This data was complemented with unpublished analyses of OC ($n = 193$), TN ($n = 235$), $\delta^{13}\text{C}$ ($n = 131$), $\Delta^{14}\text{C}$ ($n = 246$), and sediment surface area ($n = 157$) (Tables S1–S7 in Supporting Information S1). Since querying the database can lead to multiple sampling sections derived from a single core (i.e., 0–1 cm, 1–2 cm), compositions in each individual sediment core were averaged to ensure that each location was represented by a single value for each parameter.

3.1.2. Predictor Features

Recently, the use of spatial machine learning to predict spatial variation of a given parameter (e.g., OC content, sedimentation rate, sediment density) has been growing (Diesing et al., 2014, 2021; Graw et al., 2021; Lee et al., 2019; Mitchell et al., 2021; Restrepo et al., 2020). Some studies apply machine learning models following a data-driven approach, utilizing as many predictor features as possible to produce the most accurate predictions (Graw et al., 2021; Lee et al., 2019; Restrepo et al., 2020), whereas others use a knowledge-driven approach by restricting predictor features to those that are known to influence the dependent variable (Diesing et al., 2021; Mitchell et al., 2021). While a data-driven approach may provide more accurate results, it does not help understand why the spatial patterns exist, since it is difficult to unravel the influence of numerous predictor features. Hence, a knowledge-driven approach was taken in the present study and specific environmental conditions that are known to drive the distribution of the studied variables were extracted from various sources, which either reflect depositional conditions, hydrodynamic processes or source of OM (Table S8 in Supporting Information S1). Temporally changing predictor features such as primary productivity and temperature were averaged over several decades to reflect baseline conditions and minimize the effect of seasonal and extreme events. All features were re-projected to an azimuthal equidistant projection (central meridian: 116.2724°E , latitude of origin: 21.05894°N) as well as re-sampled and re-aligned to the same sample grid resolution (441 m) using ArcGIS Pro v2.9.

3.2. Spatial Prediction and Determination of *Isodrapes*

Random Forest Regression is a popular non-parametric machine learning model that creates a multitude of regression trees that are then averaged to provide a response based on a series of predictor features. The model repeatedly builds trees from random subsets of training data and predictors, and the best predictor is used to partition the data (Breiman, 2001). The versatility of this machine learning algorithm relies on its non-parametric nature, which allows it to predict patterns in the absence of linear relationships between the predictor features (i.e., environmental conditions) and the response variable, which is why it has been used in numerous applications in marine geosciences (Atwood et al., 2020; Diesing et al., 2021; Mitchell et al., 2021). The modeling framework used to predict the spatial distribution of each variable is described in Figure S1 in Supporting Information S1 and summarized below.

The spatial machine learning modeling framework is divided into two sections: (a) feature selection (Figure S1a in Supporting Information S1), and (b) model training and spatial prediction (Figure S1b in Supporting Information S1). The feature selection first executes a Boruta algorithm to identify the features that are statistically more relevant than their shuffled counterpart (Kursa & Rudnicki, 2010). Features that are statistically significant are then assessed for collinearity, and the most important features are retained. Finally, using the most important

features that are not correlated between each other, a parsimonious forward feature selection is applied to retain the most important features that do not improve the test score (Figure S1a in Supporting Information S1).

In the model training and spatial prediction, a nested cross validation approach with an inner train-test split iterator ($n = 50$) and an outer train-test split iterator ($n = 50$) is employed (Figure S1b in Supporting Information S1). The inner train-test split iterator (often referred to as cross-validation iterator, hereinafter referred to as *inner-cv*) is used to train and validate the model, providing prediction surfaces, defined as a continuous numerical representation of a response variable (i.e., OC or TN content, $\delta^{13}\text{C}$, $\Delta^{14}\text{C}$, and mineral surface area) deposited along the seafloor. The outer train-test split iterator, hereinafter referred to as *outer-cv*, allows the determination of performance metrics of the model using an unseen test set as well as obtain measurements of reproducibility and uncertainties (Figure S1b in Supporting Information S1). The prediction surface for each variable was obtained from the mean predictions of the 50 iterations, whereas uncertainties of the prediction surfaces were computed as the standard deviations of these 50 iterations. Performance metrics from the test dataset of each *outer-cv* iteration were averaged and standard deviations were computed and reported for each model.

Since the dataset is spatially clustered as a consequence of separate studies focused on specific sub-regions, a normal random sampling would lead to oversampling in areas with high density of datapoints, skewing the model to overfit in that area and perform poorly in other under-sampled areas (Figure S2a in Supporting Information S1). Hence, with the aim of having the dataset independently and identically distributed, both the *outer-cv* and *inner-cv* extract spatially balanced data based on their geographical locations through a stratified sampling approach in equal-sized polygons (Figure S2b in Supporting Information S1). This guarantees that the model always trains and validates using a representational dataset from all areas, whereas the model's performance metric is obtained from an unseen test subset that is also representational of all areas.

Finally, to identify the different “*isodrapes*,” regions where sediment with similar geochemical signatures of OC, TN, OC/TN, mineral surface area, $\delta^{13}\text{C}$ and $\Delta^{14}\text{C}$ drape the seafloor, an unsupervised k-means clustering was applied on the prediction surfaces of these variables after normalizing them. The elbow approach was used to determine the optimal number of clusters. This method consists of applying the clustering algorithm using different number of clusters and quantifying the sum of squared distances of samples to their closest cluster center in each iteration. As the number of clusters increases, the variance within a cluster decreases, but the marginal benefit of increasing the number of clusters decreases as well. Therefore, the optimal number of clusters is a balance between improving the distances of the samples within a cluster and the number of clusters. In this study, the optimal number of clusters, or *isodrapes*, was found to be three.

These algorithms were developed using Python's *Scikit-learn* machine learning module (Pedregosa et al., 2011).

4. Results and Discussion

4.1. Spatial Variations in Organic Matter Quantity, Source, Age, and the Effect of Mineral Protection

Surface sediments from the East Asian marginal seas present statistically significant varying geochemical properties with distinct spatial patterns (Table S9 in Supporting Information S1). Highest OC contents occur in mud deposits ($>0.8\%$ OC, $>0.1\%$ TN, $>15\text{ m}^2\cdot\text{g}^{-1}$ mineral surface area) offshore Region II (Bao et al., 2018; Yu et al., 2022; Zhao et al., 2018), and downcurrent of the major rivers: Yellow River (Liu et al., 2015), Yangtze River (Zhao et al., 2021), Pearl River (Wei et al., 2020), and the Gulf of Thailand rivers (Bai et al., 2021; B. Lin et al., 2023), whereas lowest OC contents are found on the shallow hydrodynamic shelves (Figures 2a–2d). With respect to regional variations of OC and TN among the marginal seas, Region I exhibits generally lower contents ($0.37 \pm 0.20\%$ OC, $0.051 \pm 0.022\%$ TN) and Region II ($0.51 \pm 0.33\%$ OC, $0.072 \pm 0.051\%$ TN), whereas higher contents were observed in Region VI ($0.75 \pm 0.5\%$ OC, $0.11 \pm 0.06\%$ TN), and Region VII ($0.74 \pm 0.33\%$ OC, $0.10 \pm 0.04\%$ TN) (Figures 3a and 3b). A higher mineral surface area was observed in Region VII ($20 \pm 11\text{ m}^2\cdot\text{g}^{-1}$) due to the preferential transport of fine-grained sediment to this deeper basin, along with higher OC contents that are preferentially associated with this sediment fraction (Figures 2 and 3). Other additional external factors such as the greater proportion of smectites in clays of this region (Table 1) as well as the influence of volcanic ash from the Pinatubo eruption, which affected the eastern edge of this region offshore Luzon (Wiesner et al., 2004), could increase the mineral surface area of surficial sediments in Region VII.

The spatial distribution in $\delta^{13}\text{C}$ values followed an evident trend influenced by the presence of the most important riverine discharge outflows, with lower values offshore the Yellow River (-23.2‰) (Hou et al., 2020; Liu

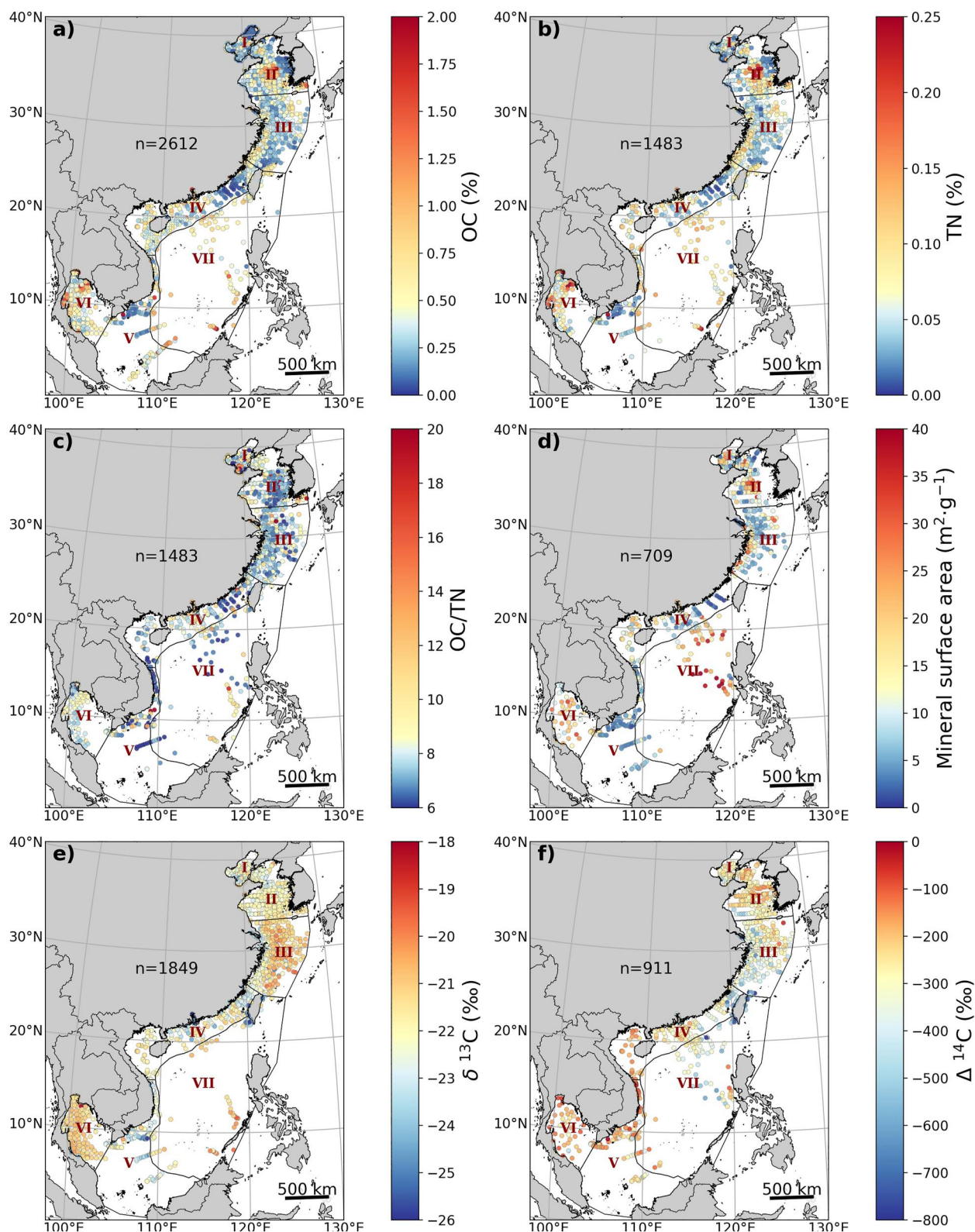


Figure 2. Distribution of main geochemical variables: (a) organic carbon, (b) total nitrogen, (c) organic carbon to nitrogen ratio, (d) mineral surface area, (e) $\delta^{13}\text{C}$, and (f) $\Delta^{14}\text{C}$. Black lines delineate the different regions.

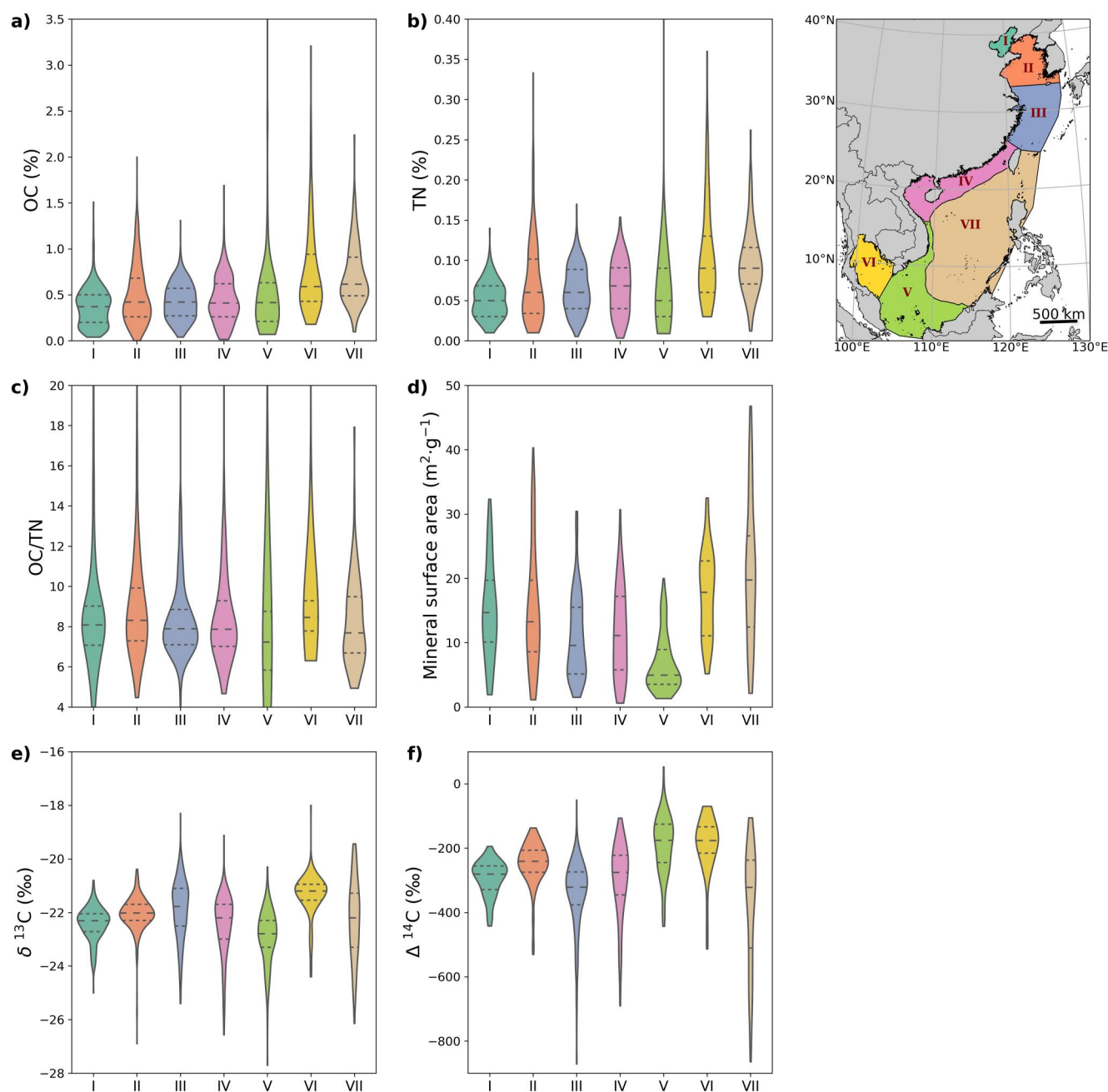


Figure 3. Violinplots of observations in each region: (a) organic carbon, (b) total nitrogen, (c) organic carbon to nitrogen ratio, (d) mineral surface area, (e) $\delta^{13}\text{C}$, and (f) $\Delta^{14}\text{C}$. The horizontal lines within the boxplots indicate the quartiles of their distribution in the regional dataset.

et al., 2015), the Yangtze River (-23.5‰) (D. Li et al., 2014; Sun et al., 2021; Y. Wu et al., 2013), the Pearl River (-24.5‰) (Hu et al., 2006; Yu et al., 2010; Zhang et al., 2014), the Mekong River (-23.8‰) (B. Lin et al., 2023; Narman, 2020), the Gulf of Thailand rivers (-23.1‰ to -28.8‰) (Bai et al., 2021; B. Lin et al., 2023; Meksumpun et al., 2005), and the Taiwanese rivers (-23.3‰) (Kao et al., 2006, 2014) (Figure 2e). The radiocarbon signature of organic carbon showed higher $\Delta^{14}\text{C}$ values in regions I, II, V, and VI, indicating the deposition of relatively fresh (younger) OC, whereas lower $\Delta^{14}\text{C}$ values were found in nearshore and distal areas of Region III, surrounding Taiwan, and in Region VII, indicating the deposition of aged OC in these deeper regions (Figures 2f and 3f).

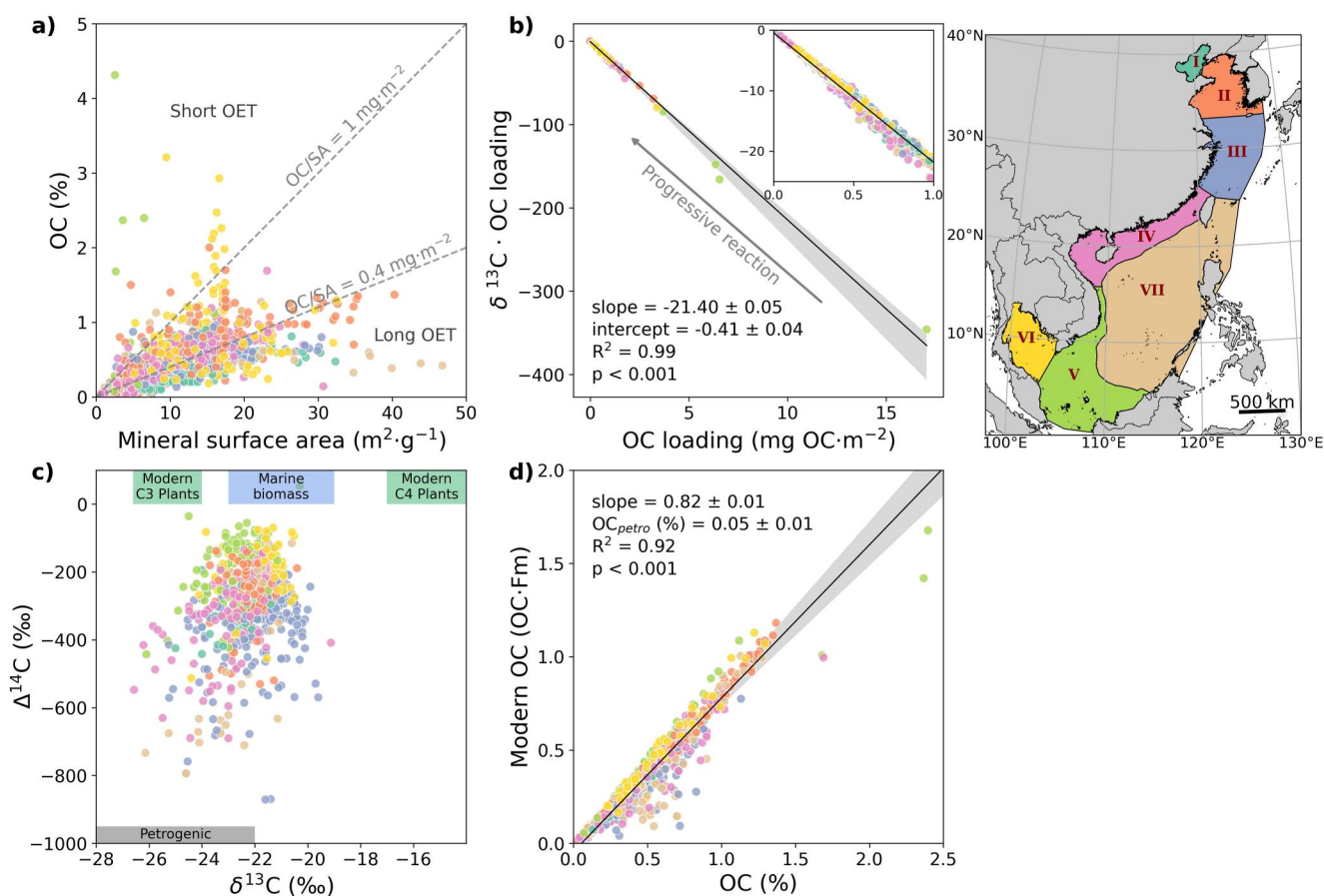


Figure 4. Correlation between different variables, with symbols color-coded according to the region they were collected: (a) OC to mineral surface area indicative of changes in OC loading, (b) relationship between OC loading and bulk stable carbon isotopic compositions ($\delta^{13}\text{C}$), (c) $\Delta^{14}\text{C}$ and $\delta^{13}\text{C}$ and potential end-members, (d) modern OC content and OC content.

Although the spatial distribution of mineral surface area and OC content follow similar patterns, there is no clear correlation between these two variables, indicative of different sedimentary OC loading properties in marine sediments in these regions (Figure 4a). Normalizing OC to mineral surface area allows for differentiation of the effects of mineral protection versus hydrodynamic particle sorting on the distribution of OC (Blair & Aller, 2012). For instance, continued sediment resuspension promotes the oxidation of OC, leading to reduced OC loadings, typically less than $0.4 \text{ mg OC} \cdot \text{m}^{-2}$, which occurs to a greatest extent in regions I, II, and III (Bao et al., 2018; Hou et al., 2020). Region VII is also characterized by low OC loadings, potentially as a consequence of the long transit time of OC until its deposition, leading to long oxygen exposure times that promote its degradation, as well as the influence of volcanic ashes close to Luzon with high mineral surface areas that may dilute OC loadings (B. Lin et al., 2024; Wiesner et al., 2004). In contrast, OC loadings between 0.4 and $1.0 \text{ mg OC} \cdot \text{m}^{-2}$ reflect a balance between the supply of OC and its degradation, and the majority of surficial sediment samples are located within this range. Finally, certain sites in shallow areas of regions V and VI present the highest OC loadings, indicating the efficient burial of OC with limited degradation (Narman, 2020). Indeed, the main source of OM in Region VI is marine productivity (Bai et al., 2021; B. Lin et al., 2023; Meksumpun et al., 2005), which, coupled with the quick transit time until deposition in the inner shelf, can lead to limited degradation of OC and its efficient storage in this region. However, repeated cycles of sediment resuspension further offshore result in intense OC degradation within this region (B. Lin et al., 2023).

Following Aller and Blair (2006), the function of OC loading to $\delta^{13}\text{C}$ shows a progressive loss of OC as observed by the decrease of OC loading, with a net loss of OC that has a $\delta^{13}\text{C}$ value of -21.4 ‰ (Figure 4b), which is characteristic of the isotopic composition of marine OM of the area (Bai et al., 2021; X. Li et al., 2012; B. Lin et al., 2023; Y. Zhang et al., 2020; B. Zhao et al., 2018). This loss confirms the preferential degradation of this

reactive OM fraction, resulting in preferential accumulation of terrestrial and petrogenic OC in this system (Fu et al., 2022; B. Lin et al., 2023; M. Yu et al., 2022; B. Zhao et al., 2021). Indeed, the relationship between $\Delta^{14}\text{C}$ and $\delta^{13}\text{C}$ values reveal that the surficial sediment with fresher OC (less depleted $\Delta^{14}\text{C}$ values) has $\delta^{13}\text{C}$ values that tend toward marine biomass endmember values, and during progressive aging, tend toward lower $\delta^{13}\text{C}$ values characteristic of terrestrial biomass or petrogenic OC discharging onto this margin (Figure 4c).

The correlation between modern OC content (the product of OC and ^{14}C expressed as fraction modern) and OC content (Figure 4d) can be used to determine the contribution of biogenic and petrogenic OC in the study area as well as the degree of OC aging due to hydrodynamic processes (Chu et al., 2022; Galy et al., 2008). The correlation between modern OC and OC content shows a statistically significant linear fit, indicating a generally similar contribution of petrogenic OC throughout the whole study area ($0.05 \pm 0.01\%$). However, this contribution must spatially vary given the contrasting contribution of petrogenic OC as well as the different degrees of aging throughout the study area. Notably, we observe a slight deviation from this linear fit toward less modern OC content in the distal areas of regions III and VII (Figure 4d), indicating a greater influence of petrogenic OC and/or the effect of aging due to resuspension cycles (Bao et al., 2018, 2019; Chu et al., 2022; B. Lin et al., 2024).

4.2. Controls on the Distribution of Organic Matter and Prediction Surfaces

The spatial prediction surfaces of OC, TN, mineral surface area, and the isotopic composition of OC ($\delta^{13}\text{C}$ and $\Delta^{14}\text{C}$) are in accordance with the spatial trends observed (Figures 2 and 5). The spatial distribution of the uncertainties of the random forest regression models was highly correlated with the spatial availability of the data, being largest in Region VII where less datapoints are available (Figure S3 in Supporting Information S1). Interestingly, large modeling uncertainties were also observed offshore the Mekong River and inner Region VI due to the marked variability of OC and TN content in the samples collected here, which may in turn possibly reflect seasonal or interannual variations in OM quantity and composition delivered by these rivers (Ellis et al., 2012; B. Lin et al., 2023; B. Wu et al., 2020). The distribution of the models' residuals did not follow a spatial trend, an indication of its unbiased performance (Figures S4a–S8a in Supporting Information S1). However, the models consistently overestimated at the lower ends and underestimated at the higher ends, given the lack of sufficient observational data to train the models in these extreme values. Nevertheless, the variance explained by the predicted values ranged between 75% and 92% (R^2 in Figures S4b–S8b in Supporting Information S1), comparable to other machine learning modeling studies (Atwood et al., 2020; Diesing et al., 2021; Graw et al., 2021; Mitchell et al., 2021; Restrepo et al., 2020). However, this metric is not an indication of the models' prediction capacity since it is calculated using the whole dataset, including the data used to train the model, leading to an overly optimistic and unrealistic metric. Instead, a proper prediction metric should be derived from an unseen dataset. Hence, we also reported the average variance explained by unseen datasets (test datasets of the *outer-cv*, see 3.2 for more details), which ranged between 46% and 92%, an indication of the models' capacity of predicting trends in the distribution of geochemical properties of surface sediments (Table S10 in Supporting Information S1).

The Random Forest Regression models accurately predicted the mudbelts with high OC and TN contents ($>0.8\%$ OC, $>0.1\%$ TN), and high mineral surface area ($>15 \text{ m}^2\cdot\text{g}^{-1}$) in regions I, II, III, and VI, as well as those located downcurrent the Yangtze and Pearl rivers (Figures 5a, 5b, and 5d). Interestingly, similarly high values of OC, TN, and even higher values of mineral surface area ($>30 \text{ m}^2\cdot\text{g}^{-1}$) were predicted in Region VII as a result of winnowing of OC-rich fine-grained sediment from the basin flanks and focusing into this distal basin. In contrast, the continental shelves generally presented lower OC and TN contents as well as lower mineral surface area, an indication that these highly dynamic shelves prevent the deposition of fine-grained sediment with high OM contents, promoting its along-, and off-shore dispersal and degradation until its final deposition in Region VII.

The distributions of OC, TN, and mineral surface area were governed by similar predictor features (Figures S4d–S6d in Supporting Information S1), which is expected given the close relationship between these properties. Bottom temperature was the most important predictor feature for these three variables. While bottom temperature can be a depositional process that regulates the remineralization of OM (Burdige, 2011; Jin & Bethke, 2005), it is classified here as a factor reflecting hydrodynamic processes due to the presence of several temperature-driven eddies in this margin. Indeed, cold-water eddies promote the formation of stable mud deposits, whereas warmer bottom waters stimulate the remineralization of OM (Guo et al., 2021; B. Zhao et al., 2018). Similarly, surface water concentrations of key nutrients such as silicate, nitrate, calcite and iron were important predictor

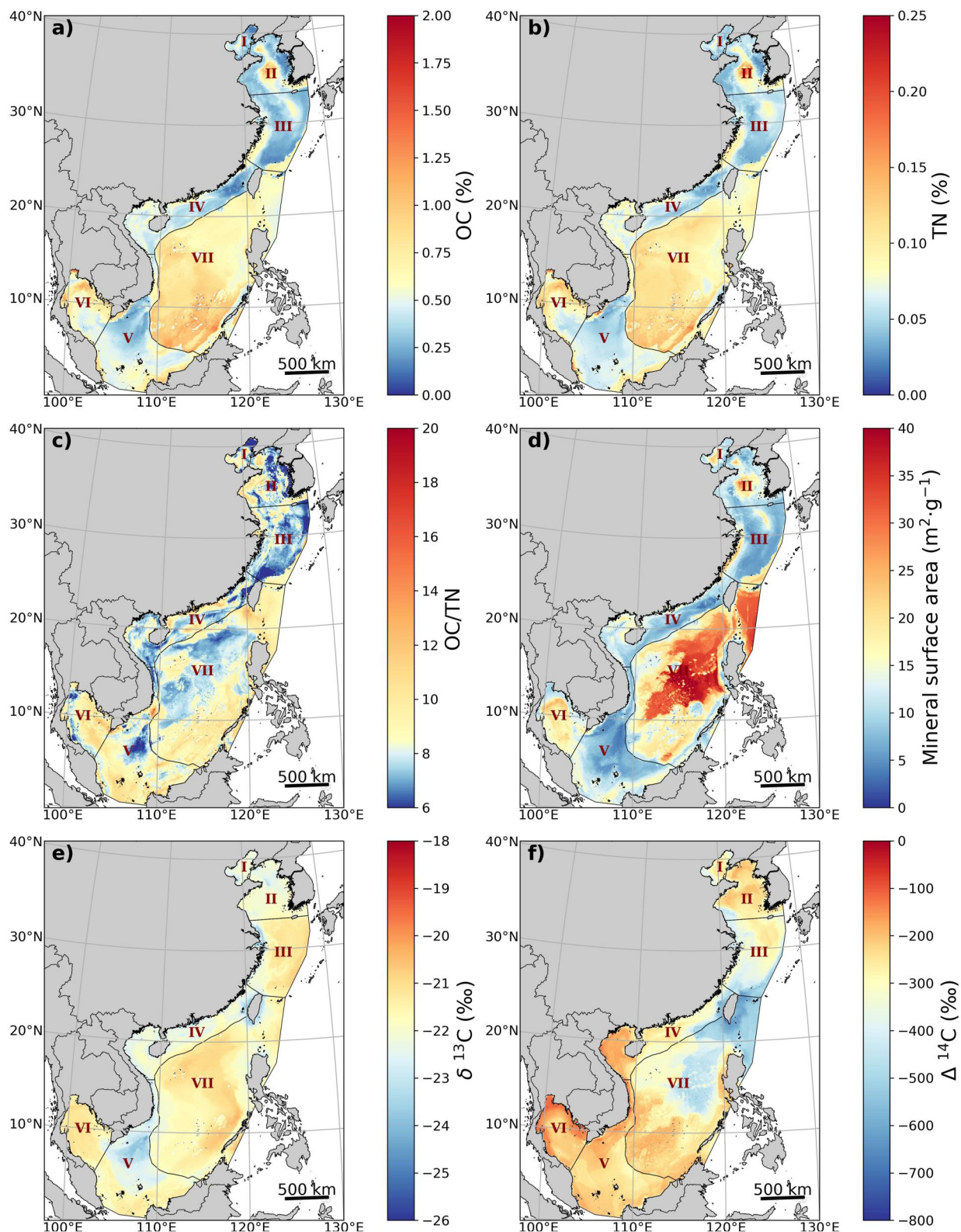


Figure 5. Prediction surfaces of main geochemical properties: (a) organic carbon, (b) total nitrogen, (c) organic carbon to nitrogen ratio, (d) mineral surface area, (e) $\delta^{13}\text{C}$, and (f) $\Delta^{14}\text{C}$. The OC to TN ratio surface is not modeled but is instead computed using the prediction surface of OC (a) and total nitrogen (b). Errors derived from the prediction surfaces can be found in Figure S3 in Supporting Information S1, whereas prediction metrics for each variable are in Figures S4–S8 in Supporting Information S1.

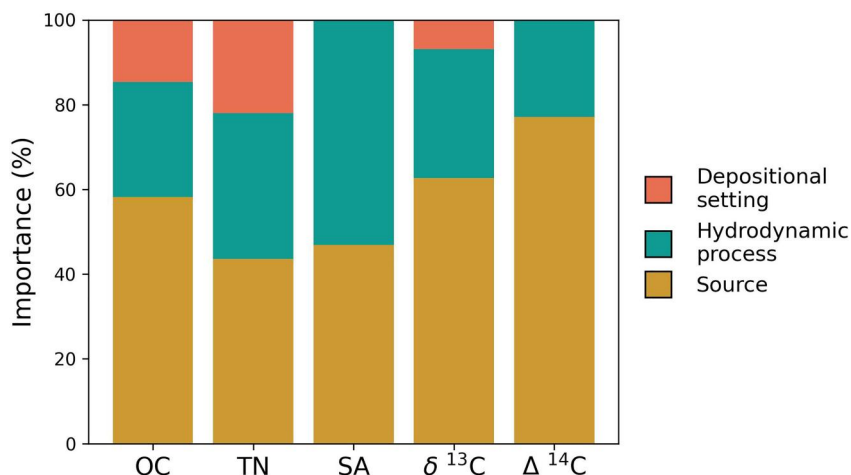


Figure 6. Relative importance of environmental factors (hydrodynamic processes, OM source, and depositional setting) that modulate the distribution of: (a) organic carbon, (b) total nitrogen, (c) mineral surface area, (d) $\delta^{13}\text{C}$, and (e) $\Delta^{14}\text{C}$. Refer to Table S8 in Supporting Information S1 for the list of features classified into each environmental factor.

features in the distribution of these variables (Figures S4d and S5d in Supporting Information S1) given their role in both the production and preservation of OM in marine sediments. Interestingly, surface silicate concentrations were more important in predicting the distribution of OC and TN in comparison to surface calcite (Figures S4d and S5d in Supporting Information S1), which is related to the mainly diatomaceous origin of OM relative to calcareous origin (Chen, Hu, Yang, & Gao, 2021; Chen, Hu, Yang, Gao, & Zhou, 2021; D. Liu et al., 2015). Finally, bottom oxygen concentration was also important in predicting the distribution of OC and TN, since reduced oxygen exposure promotes the preservation of OM (Arnarson & Keil, 2007; Hartnett et al., 1998; LaRowe et al., 2020). Overall, factors associated with source explained 44%–58% of the distribution of OC and TN, hydrodynamic processes explained 27%–34% of their distribution, and depositional conditions explained the remaining 15%–22% of the distribution. In contrast, the distribution of mineral-specific surface area was relatively equally explained by factors associated with source (53%) and hydrodynamic processes (47%) (Figure 6).

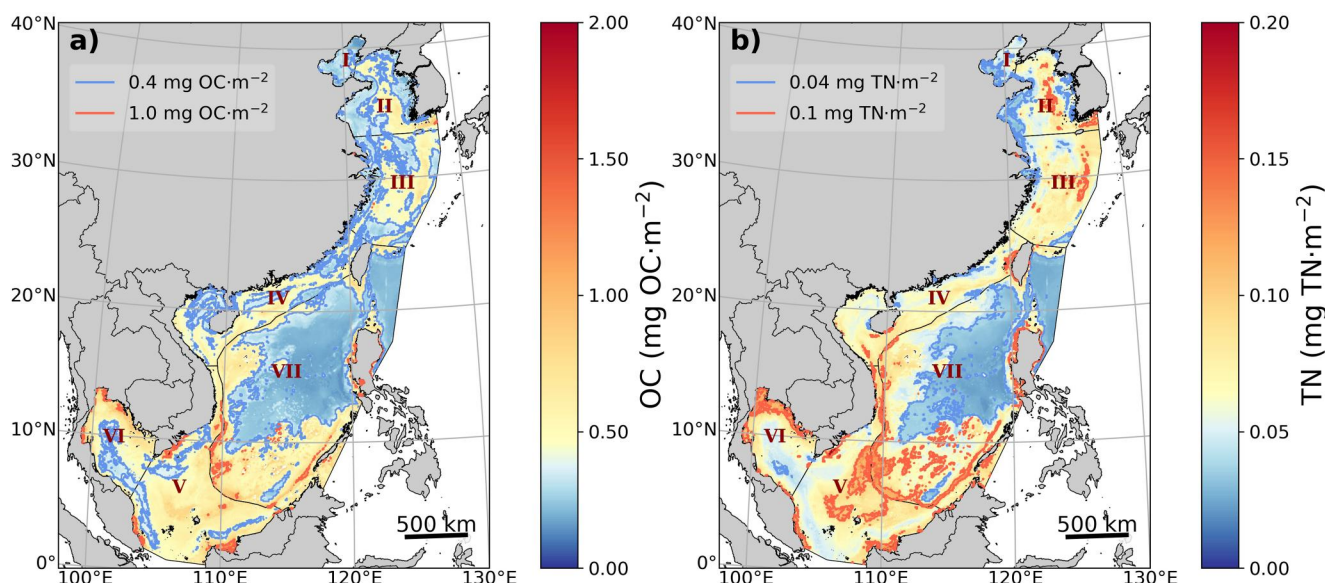


Figure 7. Spatial distribution of OC (a) and TN (b) loadings (contents normalized by the sediment surface area). Contour lines define the boundary of specific OC and TN loadings.

The normalization of OC and TN contents to mineral surface area is a further indication of the preservation or degradation potential of OM in marine sediments (Figure 7). While OC loading tends to decrease with distance from shore due to the degradation of OC during its transit time (Blair & Aller, 2012), the spatial distribution of OC loading sometimes indicates higher loadings offshore (Figure 7a). This contrasting trend has been attributed to the binding of marine OM to mineral surfaces in surficial marine sediments (Y. Wu et al., 2013), as supported by enhanced concentrations of algal-derived organic carbon (D. Liu et al., 2015). Interestingly, mud deposits presented different OC loadings, supporting previous findings that certain mud-rich settings act as incinerators of OC, whereas others stabilize OC and promote its burial (B. Zhao et al., 2018). For instance, the mud belt downcurrent from the Yangtze River has an OC loading $<0.4 \text{ mg OC}\cdot\text{m}^{-2}$, which confirms that this transient deposit enhances the remineralization of OC, whereas the OC loading $>0.4 \text{ mg OC}\cdot\text{m}^{-2}$ in the mud deposit of the southern Region II implies that OM is efficiently buried here due to the cold water masses that stabilize sedimentary environments (Guo et al., 2021; Yao et al., 2014; M. Yu et al., 2022; B. Zhao et al., 2018). Interestingly, while Region VII is characterized by high OC and TN contents (Figures 5a and 5b), this area actually has low OC and TN loadings (Figure 7), an indication that fine grained sediments accumulating in this deep basin have been intensively reworked and associated OM has been remineralized during its long transit time until its deposition.

Despite the similar spatial trends of OC and TN, the OC/TN ratio varied in the East Asian marginal seas due to contrasting contributions of terrestrial and marine OM in the system. OC/TN values close to the Redfield ratio (OC/TN = 6–7) were observed in the distal area of regions II, III, and V and in the deeper Region VII, presumably due to the greater influence of marine OM in comparison to terrestrial OM in these areas, whereas higher values were observed close to shore (Figure 5c).

The prediction surface of $\delta^{13}\text{C}$ was largely homogenous, averaging -22 ‰ throughout the study area (Figure 5e). Lower $\delta^{13}\text{C}$ values (-24 to -26 ‰) were observed along the dispersal pathway of the Yellow River, Yangtze River, Taiwanese rivers, Pearl River, Red River and the Mekong River, in agreement with the spatial trends in the observations (Figures 3e and 5e). Indeed, source of OM dominated the distribution of $\delta^{13}\text{C}$ signatures across this margin, explaining 63% of its distribution (Figure 6), since the most influential predictor features in these models were the downcurrent distance from river mouths and surface chlorophyll concentrations given their respective relationships to terrestrial and marine OM inputs and hence the signature of $\delta^{13}\text{C}$ accumulating in marine sediments (Figure S7c in Supporting Information S1; Hou et al., 2020; J. Hu et al., 2006; Kao et al., 2003; Wei et al., 2020; Xing et al., 2011; Yao et al., 2015; F. Yu et al., 2010; Y. Zhang et al., 2014).

Finally, the prediction surface of $\Delta^{14}\text{C}$ illustrates the effect of both provenance (77%) and hydrodynamic processes (23%) on the age of OC accumulating in surface sediments of this marginal sea system (Figures 5f and 6) (Bao & Blattmann, 2020). Sedimentary OC can either originate from young marine biomass, from pre-aged (^{14}C -depleted) terrestrial OM, or from petrogenic (and thus ^{14}C -free) OC. Accordingly, the Random Forest Regression model predicted higher $\Delta^{14}\text{C}$ values in areas dominated by marine productivity, whereas lower $\Delta^{14}\text{C}$ values were found downcurrent from certain rivers, indicating the dispersal of pre-aged terrestrial and/or fossil petrogenic OM. This was the case for sediments downcurrent the Yellow River in Region I (-350 ‰), downcurrent the Yangtze River in Region III (-400 ‰) but not offshore the Pearl River, Mekong River, or the rivers that discharge into the Gulf of Thailand, consistent with the contrasting age of OC discharged by these different river systems (Hou et al., 2021; B. Lin et al., 2023; Tao et al., 2018; X. Wang et al., 2012; M. Yu et al., 2019). Even more aged OC ($\Delta^{14}\text{C} = -700 \text{ ‰}$) was predicted surrounding Taiwan due to the strong influence of petrogenic OC eroded from bedrock by the mountainous rivers of the island (B. Lin et al., 2020). This trend is more evident south of Taiwan than to the northwest, in agreement with the spatial variation of the isotopic composition of the numerous rivers that discharge from this island (B. Lin et al., 2020), while the presence of submarine canyons allows an efficient offshore dispersal of petrogenic OC to the deeper Region VII (Kao et al., 2014; Sparkes et al., 2015). The effect of OC provenance on the distribution of $\Delta^{14}\text{C}$ values is further confirmed by the predictor features of the model. Predictor features representing both marine (e.g., surface ocean silicate, iron and chlorophyll concentrations) and terrestrial (e.g., downcurrent distance from rivers and the closest river) origins were the most important for the distribution of $\Delta^{14}\text{C}$ values (Figure S8c in Supporting Information S1). Identifying which is the closest river was relevant in modeling the distribution of $\Delta^{14}\text{C}$, whereas the distribution of $\delta^{13}\text{C}$ was mainly dependent on the downcurrent distance from rivers, irrespective of which river (Figures S7c and S8c in Supporting Information S1). Indeed, the variations in the isotopic signature of OC discharged by rivers in the East Asian marginal seas are mostly driven by the variations in $\Delta^{14}\text{C}$ rather than $\delta^{13}\text{C}$ (Hou et al., 2021; Kao et al., 2014; B. Lin et al., 2020; Tao et al., 2018; Wang et al., 2012; Yu et al., 2019).

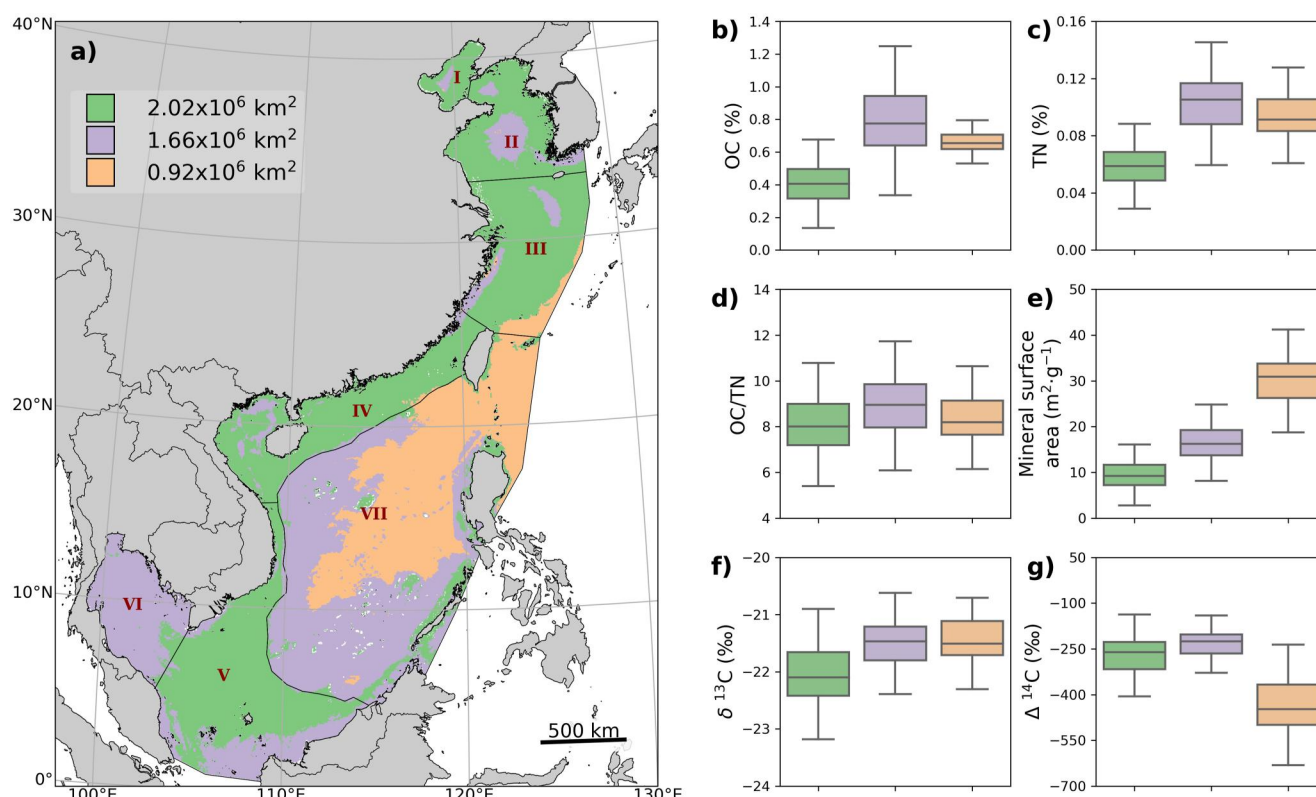


Figure 8. Regionalization of similar geochemical properties draping the seafloor (*isodrapes*) and their spatial extent (a). Geochemical composition of each isodrape: (b) organic carbon, (c) total nitrogen, (d) organic carbon to nitrogen ratio, (e) mineral surface area, (f) $\delta^{13}\text{C}$, and (g) $\Delta^{14}\text{C}$.

Hydrodynamic processes can also affect the aging of OC, where repeated cycles of sediment resuspension and redeposition during its transport lead to the preferential degradation of young and reactive OC, promoting the aging of residual OC (Bao et al., 2016, 2018). This contributes to an offshore aging evident only in the broad shelf of Region III but not in the narrow shelves of regions IV and V, given the limited transit time in these latter regions (Bao et al., 2016, 2018; Narman, 2020). Finally, long oxygen exposure time during the transport of sediment, which promotes the degradation of young and reactive OC, leads to the deposition of even older OC in the deep Region VII (B. Lin et al., 2024), the final receptacle of particulate matter in area (Figure 5f). This is confirmed by the fact that downcurrent distance from shore and depth are important features modeling the distribution of $\Delta^{14}\text{C}$ (Figure S8d in Supporting Information S1). In addition, sedimentation rates in this region are the lowest (Table 1), so surficial sediment sampled in the upper centimeters would encompass hundreds or even thousands of years, where radioactive decay could further lower $\Delta^{14}\text{C}$ values in Region VII. However, both downcurrent distance from shore and depth are less important than the features related to the provenance of OC, suggesting that the OC source is of paramount importance in modulating the OC age in surficial marine sediments in the East Asian marginal seas.

4.3. *Isodrapes*: Geochemical Regionalization of the Seafloor Sediment Drape

Through unsupervised clustering of the prediction surfaces, we identified regions that are draped by sediment with similar geochemical compositions, which we introduce here as “*isodrapes*.” These *isodrapes* can serve to identify different depositional conditions that influence the distribution of geochemical properties, such as mudbelts, or the identification of distinct habitats (Levin & Sibuet, 2012). The identification of *isodrapes* will vary depending on the scale of analysis, identifying small-scale variations when the analysis is performed at a local scale (Van der Voort et al., 2018), whereas larger-scale variations are identified in this study when performing this analysis throughout the different regions that encompass the East Asian marginal seas. Within these marginal seas, we identified three distinct *isodrapes*, which are mainly affected by variations in OC and TN

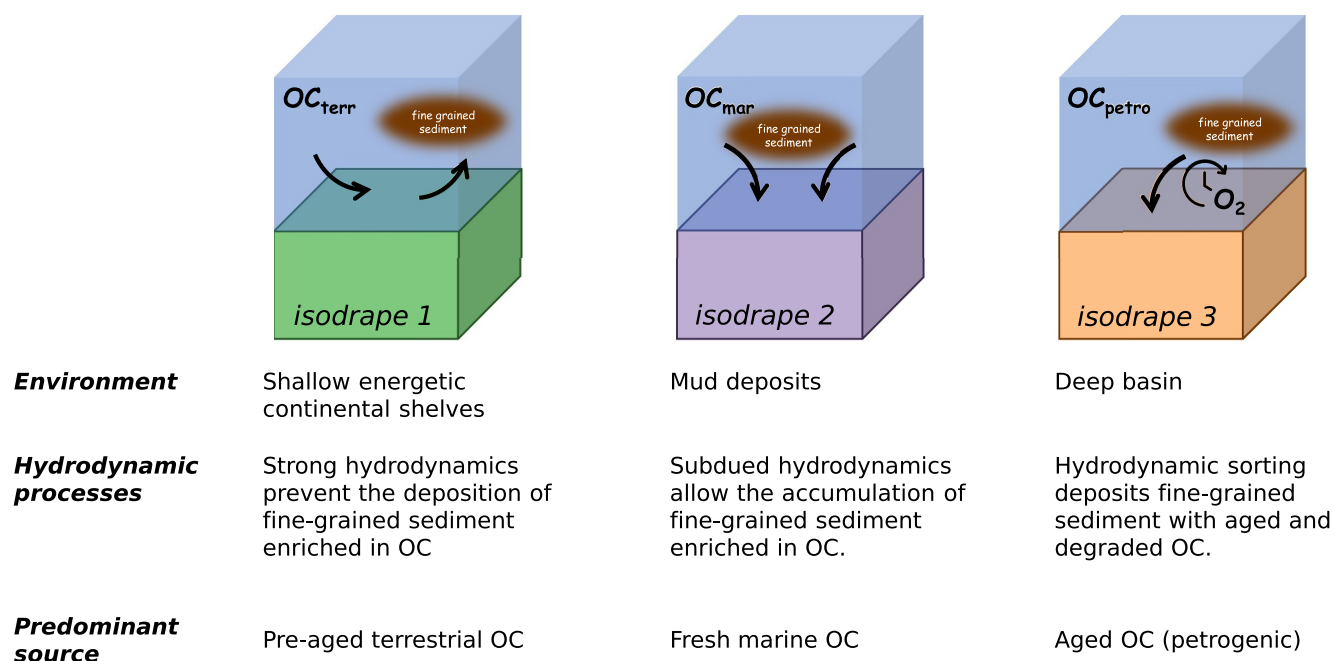


Figure 9. Schematic diagram of the general depositional environment, prevailing hydrodynamic processes and predominant source inputs that distinguish each isodrape.

content, mineral-specific surface area, and $\Delta^{14}C$, whereas the OC/TN ratio and $\delta^{13}C$ presented relatively invariant values in each isodrape (Figure 8).

The first isodrape occurs along most of the shelves and had the greatest spatial extent ($2.02 \cdot 10^6 \text{ km}^2$). This region had the lowest OC ($0.4 \pm 0.1\%$), TN ($0.06 \pm 0.01\%$), and mineral surface area ($8.0 \pm 1.5 \text{ m}^2 \cdot \text{g}^{-1}$), an indication that the hydrodynamic processes occurring along the shelf hinder the accumulation of fine-grained sediment with high OM contents. With respect to $\Delta^{14}C$ values, they ranged between -300 ‰ and -200 ‰ , reflecting the influence of pre-aged terrestrial material discharged by rivers, as confirmed by lower $\delta^{13}C$ values ($-22 \pm 2.4 \text{ ‰}$) in this region (Figures 8 and 9).

The second isodrape had a smaller spatial extent ($1.66 \cdot 10^6 \text{ km}^2$) and included the mud deposits in regions I, II, and VI, and downcurrent from the Yangtze river mouth. This region had the highest OC ($0.8 \pm 0.2\%$) and TN ($0.10 \pm 0.02\%$) contents, although the mineral surface area ($16 \pm 3 \text{ m}^2 \cdot \text{g}^{-1}$) did not present the highest values. Finally, $\Delta^{14}C$ values for this isodrape were highest ($-225 \pm 50 \text{ ‰}$), indicating the influence of fresh marine OC accumulating in these regions in comparison to the other *isodrapes* (Figures 8 and 9). This region also encompassed the upper continental slope of region VII, where diminished hydrodynamic forcing may allow the deposition of finer-grained sediment with high OM contents (Yin et al., 2019) (Figures 8 and 9).

Finally, the last isodrape had the smallest extent ($0.92 \cdot 10^6 \text{ km}^2$) and was located exclusively offshore Taiwan and in the deep Region VII (Figure 7). This region had the highest mineral surface area ($30 \pm 6 \text{ m}^2 \cdot \text{g}^{-1}$), lowest $\Delta^{14}C$ values ($-450 \pm 90 \text{ ‰}$) and average OC ($0.66 \pm 0.07\%$) and TN ($0.09 \pm 0.01\%$) contents, likely due to hydrodynamic sorting processes and the mineral-protection of OM, as well as the supply of fine-grained phyllosilicates (Z. Liu et al., 2010), leading to the deposition of sediments with a high mineral surface area and average OC and TN contents in this region. In addition, this isodrape reflects the combined effect of hydrodynamic sorting and provenance regulating the age of OC depositing in marine sediments. The preferential degradation of young OC during the transport resulted in the deposition of the most ^{14}C -depleted OC in this basin, as well as the dispersal of petrogenic OC discharged by Taiwanese rivers and funneled through the canyons incising the Taiwanese shelf (Figure 9).

4.4. Limitations and Future Directions

This study predicts the distribution of different geochemical compositions of marine sediment and identifies regions draped by sediment with similar geochemical compositions (*isodrapes*) using sparse distribution of

datapoints. From the spatial distribution of the models' uncertainties, it is evident that areas with sparse data have greater modeling uncertainties, such as in Region VII (Figure S3 in Supporting Information S1), hence more effort should be undertaken to sample and harmonize existing data from underrepresented regions. Moreover, the combined data set comprises measurements of surficial sediment cores collected during different seasons and years and thus does not account for potential natural or anthropogenically induced temporal variations. Recent studies have identified that seasonal variations can affect the geochemical composition of surficial sediment offshore estuaries (Wu et al., 2020; Zhang et al., 2020), whereas river damming has reduced the discharge of terrestrial OC over the last decades, with limited understanding of its effect on the deposition of OC in the adjacent marginal seas (Wang et al., 2022; Wu et al., 2020). In addition, considering the pervasiveness of the deposition of terrestrial OC throughout the East Asian marginal seas (Hou et al., 2021; S.-J. Kao et al., 2014; B. Lin et al., 2020, 2023; Tao et al., 2018; X. Wang et al., 2012; M. Yu et al., 2019), a proper estimation of the spatial distribution of terrestrial OC originating from different rivers is necessary. In this regard, terrestrial OM is composed of a myriad of organic compounds with different chemical compositions, diverse mineral associations, and hence contrasting reactivities, all of which affect the sequestration potential of terrestrial OM in marine sediments (B. Lin et al., 2023; Wu et al., 2013; B. Zhao et al., 2021). Hence, future studies should consider potential temporal variations in OM accumulating in this highly complex continental marginal sea system as well as delineating the spatial distribution of different terrestrial OM sources discharged by different rivers. In order to conduct these spatiotemporal analyses, efforts should be directed to compile and harmonize existing datasets published both in peer-reviewed journals as well as gray literature (Paradis et al., 2023), which will allow similar regional studies addressing the distribution of OM content, origin, and quality in other continental margins.

5. Conclusions

We applied spatial machine learning models to understand the factors that affect the distribution of organic matter content, composition and age in an expansive, highly complex continental margin setting. Our findings demonstrate that the fate of organic matter in the East Asian marginal seas is primarily governed by a combination of hydrodynamic processes and provenance. Sediment dispersal mechanisms promote the formation of mud deposits where either intense degradation organic matter or its burial occurs, whereas winnowing of fine-grained sediment enriched in organic matter in the shallow marginal seas leads to the dispersal and eventual deposition of aged and degraded organic matter toward deeper regions. This process is coupled with contrasting isotopic compositions of organic matter discharged by diverse rivers draining onto this margin, regulating the spatial distribution of organic matter deposited in the East Asian margin.

We also identify three main regions where sediment with distinct geochemical properties drape the seafloor (*isodrapes*) in the East Asian margin: (a) the continental shelf with coarser-grained sediments hosting pre-aged low organic matter that reflects both the influence of rivers and hydrodynamic processes that limit its deposition, (b) mud areas with fine-grained sediment enriched in organic matter, and (c) a distal basin with fine-grained sediment largely comprised of degraded and aged organic matter that has experienced numerous cycles of resuspension and deposition during sediment transport, as well as petrogenic organic carbon discharged by Taiwan and funneled through submarine canyons. Overall, this study shows the potential of machine learning techniques to identify processes occurring in a large and complex marine environment.

Data Availability Statement

The data used to produce this study can be accessed through MOSAIC v.2.0 (Paradis et al., 2023), and the unpublished dataset will be made available in MOSAIC once the manuscript is accepted. The code used to produce this study can be accessed through <https://doi.org/10.5281/zenodo.10781251>.

References

- Alexander, C., DeMaster, D., & Nittrouer, C. (1991). Sediment accumulation in a modern epicontinental-shelf setting: The Yellow Sea. *Marine Geology*, 98(1), 51–72. [https://doi.org/10.1016/0025-3227\(91\)90035-3](https://doi.org/10.1016/0025-3227(91)90035-3)
- Aller, R. C., & Blair, N. E. (2006). Carbon remineralization in the Amazon–Guianas tropical mobile mudbelt: A sedimentary incinerator. *Continental Shelf Research*, 26(17–18), 2241–2259. <https://doi.org/10.1016/j.csr.2006.07.016>
- Amerson, T. S., & Keil, R. G. (2007). Changes in organic matter–mineral interactions for marine sediments with varying oxygen exposure times. *Geochimica et Cosmochimica Acta*, 71(14), 3545–3556. <https://doi.org/10.1016/j.gca.2007.04.027>
- Assis, J., Tyberghein, L., Bosch, S., Verbruggen, H., Serrão, E. A., De Clerck, O., & Tittensor, D. (2018). Bio-ORACLE v2.0: Extending marine data layers for bioclimatic modelling. *Global Ecology and Biogeography*, 27(3), 277–284. <https://doi.org/10.1111/geb.12693>

Acknowledgments

This study was funded by the Swiss National Science Foundation funded project Climate and Anthropogenic PerturbationS of Land-Ocean Carbon TracKs (CAPS-LOCK3, SNF200020_184865/1; CAPS-LOCK⁺, SNF200020_215163), the National Natural Science Foundation of China (No. 42230412, 42106061), the National Research Foundation of Korea (NRF) Grants (2016R1A2B3015388 and 2021M3I6A1091270). MGW and KS acknowledge funding from the German Ministry for Education and Research (Grants 03G0132, 03G0140 and 03G0187, 03G0220) for the sediment sampling programme of the Gulf of Tonkin, Sunda Shelf and Vietnam shelf (Regions IV and V). TW received funding from the Heriot-Watt University EGIS Seed Corn Funds to support LN and her research on the Vietnamese and Sunda shelf sediments (Regions IV and V). We would also like to acknowledge Daun Kim for his contribution processing samples of the Yellow Sea (Region II), and Thomas Blattmann for his contribution processing samples of the deep South China Sea (Region VII). This manuscript has greatly benefitted from the contribution of Philip Pika, three anonymous reviewers, and the Associate Editor, whose comments and questions have improved the clarity of the manuscript. Open access funding provided by Eidgenössische Technische Hochschule Zurich.

- Atwood, T. B., Witt, A., Mayorga, J., Hammill, E., & Sala, E. (2020). Global patterns in marine sediment carbon stocks. *Frontiers in Marine Science*, 7. <https://doi.org/10.3389/fmars.2020.00165>
- Ausin, B., Bossert, G., Krake, N., Paradis, S., Haghypour, N., Durrieu de Madron, X., et al. (2023). Sources and fate of sedimentary organic matter in the Western Mediterranean Sea. *Global Biogeochemical Cycles*, 37(10), e2023GB007695. <https://doi.org/10.1029/2023GB007695>
- Ausin, B., Bruni, E., Haghypour, N., Welte, C., Bernasconi, S. M., & Eglinton, T. I. (2021). Controls on the abundance, provenance and age of organic carbon buried in continental margin sediments. *Earth and Planetary Science Letters*, 558, 116759. <https://doi.org/10.1016/j.epsl.2021.116759>
- Bai, Y., Hu, L., Wu, B., Qiao, S., Fan, D., Liu, S., et al. (2021). Impact of source variability and hydrodynamic forces on the distribution, transport, and burial of sedimentary organic matter in a tropical coastal margin: The Gulf of Thailand. *Journal of Geophysical Research: Biogeosciences*, 126(9), e2021JG006434. <https://doi.org/10.1029/2021JG006434>
- Bao, R., & Blattmann, T. M. (2020). Radiocarbonscapes of sedimentary organic carbon in the East Asian Seas. *Frontiers in Marine Science*, 7. <https://doi.org/10.3389/fmars.2020.00517>
- Bao, R., Blattmann, T. M., McIntyre, C., Zhao, M., & Eglinton, T. I. (2019). Relationships between grain size and organic carbon 14C heterogeneity in continental margin sediments. *Earth and Planetary Science Letters*, 505, 76–85. <https://doi.org/10.1016/j.epsl.2018.10.013>
- Bao, R., McIntyre, C., Zhao, M., Zhu, C., Kao, S.-J., & Eglinton, T. I. (2016). Widespread dispersal and aging of organic carbon in shallow marginal seas. *Geology*, 44(10), 791–794. <https://doi.org/10.1130/G37948.1>
- Bao, R., van der Voort, T. S., Zhao, M., Guo, X., Montluçon, D. B., McIntyre, C., & Eglinton, T. I. (2018). Influence of hydrodynamic processes on the fate of sedimentary organic matter on continental margins. *Global Biogeochemical Cycles*, 32(9), 1420–1432. <https://doi.org/10.1029/2018GB005921>
- Bezrukov, P. L., Petelin, V. P., Lisitzin, A. P., Ostroumov, E. A., Romankevich, E. A., & Skorniyakova, N. S. (1970). (Supplement 2) contents of CaCO₃, amorphous SiO₂, organic carbon, Fe, and Mn in the surface sediment layer of the Pacific Ocean: R/V Vityaz and Ob data. In Supplement to: Bezrukov, Panteleimon L.; Lisitzin, Alexander P.; Petelin, Veniamin P.; Skorniyakova, Nadezhda S.; Romankevich, Evgeny A.; Ostroumov, Esper A.; Andrushchenko, Polina F.; Volkov, Igor I (1970). In P. L. Bezrukov (Ed.), *Sedimentation in the Pacific Ocean. Part 2. Pacific Ocean monogr* (p. 419). PANGAEA. Nauka Publ. <https://doi.org/10.1594/PANGAEA.740038>
- Bianchi, T. S., Cui, X., Blair, N. E., Burdige, D. J., Eglinton, T. I., & Galy, V. (2018). Centers of organic carbon burial and oxidation at the land-ocean interface. *Organic Geochemistry*, 115, 138–155. <https://doi.org/10.1016/j.orggeochem.2017.09.008>
- Blair, N. E., & Aller, R. C. (2012). The fate of terrestrial organic carbon in the marine environment. *Annual Review of Marine Science*, 4(1), 401–423. <https://doi.org/10.1146/annurev-marine-120709-142717>
- Blattmann, T. M., Liu, Z., Zhang, Y., Zhao, Y., Haghypour, N., Montluçon, D. B., et al. (2019). Mineralogical control on the fate of continentally derived organic matter in the ocean. *Science*, 366(6466), 742–745. <https://doi.org/10.1126/science.aax5345>
- Blattmann, T. M., Zhang, Y., Zhao, Y., Wen, K., Lin, S., Li, J., et al. (2018). Contrasting fates of petrogenic and biospheric carbon in the South China Sea. *Geophysical Research Letters*, 45(17), 9077–9086. <https://doi.org/10.1029/2018GL079222>
- Boonyatumanond, R., Wattayakorn, G., Amano, A., Inouchi, Y., & Takada, H. (2007). Reconstruction of pollution history of organic contaminants in the upper Gulf of Thailand by using sediment cores: First report from Tropical Asia Core (TACO) project. *Marine Pollution Bulletin*, 54(5), 554–565. <https://doi.org/10.1016/j.marpolbul.2006.12.007>
- Bouloubassi, I., Fillaux, J., & Saliot, A. (2001). Hydrocarbons in surface sediments from the Changjiang (Yangtze River) Estuary, East China Sea. *Marine Pollution Bulletin*, 42(12), 1335–1346. [https://doi.org/10.1016/S0025-326X\(01\)00149-7](https://doi.org/10.1016/S0025-326X(01)00149-7)
- Breiman, L. (2001). Random forests. *Machine Learning*, 45(1), 5–32. <https://doi.org/10.1023/A:1010933404324>
- Bröder, L., Tesi, T., Andersson, A., Eglinton, T. I., Semiletov, I. P., Dudarev, O. V., et al. (2016). Historical records of organic matter supply and degradation status in the East Siberian Sea. *Organic Geochemistry*, 91, 16–30. <https://doi.org/10.1016/j.orggeochem.2015.10.008>
- Burdige, D. J. (2011). Temperature dependence of organic matter remineralization in deeply-buried marine sediments. *Earth and Planetary Science Letters*, 311(3–4), 396–410. <https://doi.org/10.1016/j.epsl.2011.09.043>
- Cai, G., Miao, L., Chen, H., Sun, G., Wu, J., & Xu, Y. (2013). Grain size and geochemistry of surface sediments in northwestern continental shelf of the South China Sea. *Environmental Earth Sciences*, 70(1), 363–380. <https://doi.org/10.1007/s12665-012-2133-x>
- Calvert, S., Pedersen, T., & Thunell, R. (1993). Geochemistry of the surface sediments of the Sulu and South China Seas. *Marine Geology*, 114(3–4), 207–231. [https://doi.org/10.1016/0025-3227\(93\)90029-U](https://doi.org/10.1016/0025-3227(93)90029-U)
- Chen, Y., Hu, C., Yang, G., Gao, X., & Zhou, L. (2021). Variation and reactivity of organic matter in the surface sediments of the changjiang estuary and its adjacent East China Sea. *Journal of Geophysical Research: Biogeosciences*, 126(1). <https://doi.org/10.1029/2020JG005765>
- Chen, Y., Hu, C., Yang, G.-P., & Gao, X.-C. (2021). Source, distribution and degradation of sedimentary organic matter in the South Yellow Sea and East China Sea. *Estuarine, Coastal and Shelf Science*, 255, 107372. <https://doi.org/10.1016/j.ecss.2021.107372>
- Chen, Z., Saito, Y., Kanai, Y., Wei, T., Li, L., Yao, H., & Wang, Z. (2004). Low concentration of heavy metals in the Yangtze estuarine sediments, China: A diluting setting. *Estuarine, Coastal and Shelf Science*, 60(1), 91–100. <https://doi.org/10.1016/j.ecss.2003.11.021>
- Cho, H. G., Kim, S.-O., Kwak, K. Y., Choi, H., & Khim, B.-K. (2015). Clay mineral distribution and provenance in the Heuksan mud belt, Yellow Sea. *Geo-Marine Letters*, 35(6), 411–419. <https://doi.org/10.1007/s00367-015-0417-3>
- Chu, M., Zhao, M., Eglinton, T. I., & Bao, R. (2022). Differentiating the causes of aged organic carbon in marine sediments. *Geophysical Research Letters*, 49(5), e2021GL096912. <https://doi.org/10.1029/2021GL096912>
- DeMaster, D. J., McKee, B. A., Nittrouer, C. A., Jiangchu, Q., & Guodong, C. (1985). Rates of sediment accumulation and particle reworking based on radiochemical measurements from continental shelf deposits in the East China Sea. *Continental Shelf Research*, 4(1–2), 143–158. [https://doi.org/10.1016/0278-4343\(85\)90026-3](https://doi.org/10.1016/0278-4343(85)90026-3)
- Diesing, M., Green, S. L., Stephens, D., Lark, R. M., Stewart, H. A., & Dove, D. (2014). Mapping seabed sediments: Comparison of manual, geostatistical, object-based image analysis and machine learning approaches. *Continental Shelf Research*, 34, 107–119. <https://doi.org/10.1016/j.csr.2014.05.004>
- Diesing, M., Thorsnes, T., & Bjarnadóttir, L. R. (2021). Organic carbon densities and accumulation rates in surface sediments of the North Sea and Skagerrak. *Biogeosciences*, 18(6), 2139–2160. <https://doi.org/10.5194/bg-18-2139-2021>
- Dou, Y., Li, J., Zhao, J., Wei, H., Yang, S., Bai, F., et al. (2014). Clay mineral distributions in surface sediments of the Liaodong Bay, Bohai Sea and surrounding river sediments: Sources and transport patterns. *Continental Shelf Research*, 73, 72–82. <https://doi.org/10.1016/j.csr.2013.11.023>
- Ellis, E. E., Keil, R. G., Ingalls, A. E., Richey, J. E., & Alin, S. R. (2012). Seasonal variability in the sources of particulate organic matter of the Mekong River as discerned by elemental and lignin analyses. *Journal of Geophysical Research*, 117(G1), G01038. <https://doi.org/10.1029/2011JG001816>
- Fang, G. H. (1998). A survey of studies on the South China Sea upper ocean circulation. *Acta Oceanographica Taiwanica*, 37(1), 1–16.

- Fu, W., Xu, X., Druffel, E. M., Wang, X., Sun, S., Luo, C., et al. (2022). Carbon isotopic constraints on the degradation and sequestration of organic matter in river-influenced marginal sea sediments. *Limnology & Oceanography*, 67(S2). <https://doi.org/10.1002/lno.12070>
- Galy, V., Beyssac, O., France-Lanord, C., & Eglinton, T. (2008). Recycling of graphite during Himalayan erosion: A geological stabilization of carbon in the crust. *Science*, 322(5903), 943–945. <https://doi.org/10.1126/science.1161408>
- GEBCO Compilation Group. (2022). GEBCO 2022 grid. <https://doi.org/10.5285/e0f0bb80-ab44-2739-e053-6c86abc0289c>
- Goñi, M. A., O'Connor, A. E., Kuzyk, Z. Z., Yunker, M. B., Gobeil, C., & Macdonald, R. W. (2013). Distribution and sources of organic matter in surface marine sediments across the North American Arctic margin. *Journal of Geophysical Research: Oceans*, 118(9), 4017–4035. <https://doi.org/10.1002/jgrc.20286>
- Gordon, E. S., & Goñi, M. A. (2003). Sources and distribution of terrigenous organic matter delivered by the Atchafalaya River to sediments in the northern Gulf of Mexico. *Geochimica et Cosmochimica Acta*, 67(13), 2359–2375. [https://doi.org/10.1016/S0016-7037\(02\)01412-6](https://doi.org/10.1016/S0016-7037(02)01412-6)
- Graw, J. H., Wood, W. T., & Phrampus, B. J. (2021). Predicting global marine sediment density using the random forest regressor machine learning algorithm. *Journal of Geophysical Research: Solid Earth*, 126(1), e2020JB020135. <https://doi.org/10.1029/2020JB020135>
- Guo, J., Yuan, H., Song, J., Li, X., Duan, L., Li, N., & Wang, Y. (2021). Evaluation of sedimentary organic carbon reactivity and burial in the Eastern China Marginal Seas. *Journal of Geophysical Research: Oceans*, 126(4), e2021JC017207. <https://doi.org/10.1029/2021JC017207>
- Harris, P. T., Macmillan-Lawler, M., Rupp, J., & Baker, E. K. (2014). Geomorphology of the oceans. *Marine Geology*, 352, 4–24. <https://doi.org/10.1016/J.MARGE0.2014.01.011>
- Hartnett, H. E., Keil, R. G., Hedges, J. I., & Devol, A. H. (1998). Influence of oxygen exposure time on organic carbon preservation in continental margin sediments. *Nature*, 391(6667), 572–575. <https://doi.org/10.1038/35351>
- Hedges, J. I., & Keil, R. G. (1995). Sedimentary organic matter preservation: An assessment and speculative synthesis. *Marine Chemistry*, 49(2–3), 81–115. [https://doi.org/10.1016/0304-4203\(95\)00008-F](https://doi.org/10.1016/0304-4203(95)00008-F)
- Hemingway, J. D., Rothman, D. H., Grant, K. E., Rosengard, S. Z., Eglinton, T. I., Derry, L. A., & Galy, V. V. (2019). Mineral protection regulates long-term global preservation of natural organic carbon. *Nature*, 570(7760), 228–231. <https://doi.org/10.1038/s41586-019-1280-6>
- Hou, P., Eglinton, T. I., Yu, M., Montluçon, D. B., Haghpour, N., Zhang, H., et al. (2021). Degradation and aging of terrestrial organic carbon within estuaries: Biogeochemical and environmental implications. *Environmental Science & Technology*, 55(15), 10852–10861. <https://doi.org/10.1021/acs.est.1c02742>
- Hou, P., Yu, M., Eglinton, T. I., Haghpour, N., Zhang, H., & Zhao, M. (2023). Contrasting sources and fates of sedimentary organic carbon in subtropical estuary-marginal sea systems. *Chemical Geology*, 638, 121692. <https://doi.org/10.1016/j.chemgeo.2023.121692>
- Hou, P., Yu, M., Zhao, M., Montluçon, D. B., Su, C., & Eglinton, T. I. (2020). Terrestrial biomolecular burial efficiencies on continental margins. *Journal of Geophysical Research: Biogeosciences*, 125(8), e2019JG005520. <https://doi.org/10.1029/2019JG005520>
- Hu, B., Li, J., Zhao, J., Wei, H., Yin, X., Li, G., et al. (2014). Late Holocene elemental and isotopic carbon and nitrogen records from the East China Sea inner shelf: Implications for monsoon and upwelling. *Marine Chemistry*, 162, 60–70. <https://doi.org/10.1016/j.marchem.2014.03.008>
- Hu, J., Peng, P., Jia, G., Mai, B., & Zhang, G. (2006). Distribution and sources of organic carbon, nitrogen and their isotopes in sediments of the subtropical Pearl River estuary and adjacent shelf, Southern China. *Marine Chemistry*, 98(2–4), 274–285. <https://doi.org/10.1016/j.marchem.2005.03.008>
- Hu, L., Guo, Z., Feng, J., Yang, Z., & Fang, M. (2009). Distributions and sources of bulk organic matter and aliphatic hydrocarbons in surface sediments of the Bohai Sea, China. *Marine Chemistry*, 113(3–4), 197–211. <https://doi.org/10.1016/j.marchem.2009.02.001>
- Hu, L., Shi, X., Bai, Y., Qiao, S., Li, L., Yu, Y., et al. (2016). Recent organic carbon sequestration in the shelf sediments of the Bohai Sea and Yellow Sea, China. *Journal of Marine Systems*, 155, 50–58. <https://doi.org/10.1016/j.jmarsys.2015.10.018>
- Hu, L., Shi, X., Guo, Z., Wang, H., & Yang, Z. (2013). Sources, dispersal and preservation of sedimentary organic matter in the Yellow Sea: The importance of depositional hydrodynamic forcing. *Marine Geology*, 335, 52–63. <https://doi.org/10.1016/j.margeo.2012.10.008>
- Hu, L., Shi, X., Yu, Z., Lin, T., Wang, H., Ma, D., et al. (2012). Distribution of sedimentary organic matter in estuarine-inner shelf regions of the East China Sea: Implications for hydrodynamic forces and anthropogenic impact. *Marine Chemistry*, 142–144, 29–40. <https://doi.org/10.1016/j.marchem.2012.08.004>
- Hu, L. M., Lin, T., Shi, X. F., Yang, Z. S., Wang, H. J., Zhang, G., & Guo, Z. G. (2011). The role of shelf mud depositional process and large river inputs on the fate of organochlorine pesticides in sediments of the Yellow and East China seas. *Geophysical Research Letters*, 38(3), L03602. <https://doi.org/10.1029/2010GL045723>
- Huh, C.-A., & Chen, H.-Y. (1999). History of lead pollution recorded in East China Sea sediments. *Marine Pollution Bulletin*, 38(7), 545–549. [https://doi.org/10.1016/S0025-326X\(98\)00111-8](https://doi.org/10.1016/S0025-326X(98)00111-8)
- Huh, C.-A., & Su, C.-C. (1999). Sedimentation dynamics in the East China Sea elucidated from 210Pb, 137Cs and 239,240 Pu. *Marine Geology*, 160(1–2), 183–196. [https://doi.org/10.1016/S0025-3227\(99\)00020-1](https://doi.org/10.1016/S0025-3227(99)00020-1)
- Jean-Michel, L., Eric, G., Romain, B.-B., Gilles, G., Angélique, M., Marie, D., et al. (2021). The copernicus global 1/12° oceanic and sea ice GLORYS12 reanalysis. *Frontiers in Earth Science*, 9. <https://doi.org/10.3389/feart.2021.698876>
- Jeng, W.-L., & Huh, C.-A. (2008). A comparison of sedimentary aliphatic hydrocarbon distribution between East China Sea and southern Okinawa Trough. *Continental Shelf Research*, 28(4–5), 582–592. <https://doi.org/10.1016/j.csr.2007.11.009>
- Jin, Q., & Bethke, C. M. (2005). Predicting the rate of microbial respiration in geochemical environments. *Geochimica et Cosmochimica Acta*, 69(5), 1133–1143. <https://doi.org/10.1016/j.gca.2004.08.010>
- Kao, S. J., Hilton, R. G., Selvaraj, K., Dai, M., Zehetner, F., Huang, J.-C., et al. (2014). Preservation of terrestrial organic carbon in marine sediments offshore Taiwan: Mountain building and atmospheric carbon dioxide sequestration. *Earth Surface Dynamics*, 2(1), 127–139. <https://doi.org/10.5194/esurf-2-127-2014>
- Kao, S. J., Lin, F. J., & Liu, K. K. (2003). Organic carbon and nitrogen contents and their isotopic compositions in surficial sediments from the East China Sea shelf and the southern Okinawa Trough. *Deep Sea Research Part II: Topical Studies in Oceanography*, 50(6–7), 1203–1217. [https://doi.org/10.1016/S0967-0645\(03\)00018-3](https://doi.org/10.1016/S0967-0645(03)00018-3)
- Kao, S. J., & Milliman, J. D. (2008). Water and sediment discharge from small mountainous rivers, Taiwan: The roles of lithology, episodic events, and human activities. *The Journal of Geology*, 116(5), 431–448. <https://doi.org/10.1086/590921>
- Kao, S. J., Shiah, F.-K., Wang, C.-H., & Liu, K.-K. (2006). Efficient trapping of organic carbon in sediments on the continental margin with high fluvial sediment input off southwestern Taiwan. *Continental Shelf Research*, 26(20), 2520–2537. <https://doi.org/10.1016/j.csr.2006.07.030>
- Keil, R. G., Tsamakis, E., Giddings, J. C., & Hedges, J. I. (1998). Biochemical distributions (amino acids, neutral sugars, and lignin phenols) among size-classes of modern marine sediments from the Washington coast. *Geochimica et Cosmochimica Acta*, 62(8), 1347–1364. [https://doi.org/10.1016/S0016-7037\(98\)00080-5](https://doi.org/10.1016/S0016-7037(98)00080-5)

- Kim, D., Kim, J.-H., Tesi, T., Kang, S., Nogarotto, A., Park, K., et al. (2022). Changes in the burial efficiency and composition of terrestrial organic carbon along the Mackenzie Trough in the Beaufort Sea. *Estuarine, Coastal and Shelf Science*, 275, 107997. <https://doi.org/10.1016/j.ecss.2022.107997>
- Kim, Y., Hong, S., Lee, J., Yoon, S. J., An, Y., Kim, M.-S., et al. (2021). Spatial distribution and source identification of traditional and emerging persistent toxic substances in the offshore sediment of South Korea. *Science of the Total Environment*, 789, 147996. <https://doi.org/10.1016/j.scitotenv.2021.147996>
- Kuehl, S. A., Fuglseth, T. J., & Thunell, R. C. (1993). Sediment mixing and accumulation rates in the Sulu and South China Seas: Implications for organic carbon preservation in deep-sea environments. *Marine Geology*, 111(1–2), 15–35. [https://doi.org/10.1016/0025-3227\(93\)90186-Y](https://doi.org/10.1016/0025-3227(93)90186-Y)
- Kursa, M. B., & Rudnicki, W. R. (2010). Feature selection with the Boruta package. *Journal of Statistical Software*, 36(11). <https://doi.org/10.18637/jss.v036.i11>
- LaRowe, D. E., Arndt, S., Bradley, J. A., Estes, E. R., Hoarfrost, A., Lang, S. Q., et al. (2020). The fate of organic carbon in marine sediments - New insights from recent data and analysis. *Earth-Science Reviews*, 204, 103146. <https://doi.org/10.1016/j.earscirev.2020.103146>
- Lee, T. R., Wood, W. T., & Phrampus, B. J. (2019). A machine learning (kNN) approach to predicting global seafloor total organic carbon. *Global Biogeochemical Cycles*, 33(1), 37–46. <https://doi.org/10.1029/2018GB005992>
- Levin, L. A., & Sibuet, M. (2012). Understanding continental margin biodiversity: A new imperative. *Annual Review of Marine Science*, 4(1), 79–112. <https://doi.org/10.1146/annurev-marine-120709-142714>
- Li, D., Yao, P., Bianchi, T. S., Zhang, T., Zhao, B., Pan, H., et al. (2014). Organic carbon cycling in sediments of the changjiang estuary and adjacent shelf: Implication for the influence of three Gorges Dam. *Journal of Marine Systems*, 139, 409–419. <https://doi.org/10.1016/j.jmarsys.2014.08.009>
- Li, X., Bianchi, T. S., Allison, M. A., Chapman, P., Mitra, S., Zhang, Z., et al. (2012). Composition, abundance and age of total organic carbon in surface sediments from the inner shelf of the East China Sea. *Marine Chemistry*, 145–147, 37–52. <https://doi.org/10.1016/j.marchem.2012.10.001>
- Liao, W., Hu, J., & Peng, P. (2018). Burial of organic carbon in the Taiwan Strait. *Journal of Geophysical Research: Oceans*, 123(9), 6639–6652. <https://doi.org/10.1029/2018JC014285>
- Lin, B., Liu, Z., Eglinton, T. I., Kandasamy, S., Blattmann, T. M., Haghipour, N., et al. (2020). Island-wide variation in provenance of riverine sedimentary organic carbon: A case study from Taiwan. *Earth and Planetary Science Letters*, 539, 116238. <https://doi.org/10.1016/j.epsl.2020.116238>
- Lin, B., Liu, Z., Eglinton, T. I., Wiesner, M. G., Blattmann, T. M., & Haghipour, N. (2024). Organic carbon sources in surface sediments on the northern South China Sea. *Journal of Geophysical Research: Biogeosciences*. <https://doi.org/10.1029/2023JG007909>
- Lin, B., Liu, Z., Zhao, M., Sompongchaiyakul, P., Zhang, H., Blattmann, T. M., et al. (2023). Compositions and sources of sedimentary organic carbon on the tropical epicontinental sea. *Geochimica et Cosmochimica Acta*, 351, 32–44. <https://doi.org/10.1016/j.gca.2023.04.030>
- Lin, L., Gao, J., Li, J., Pope, E., Zhao, D., Wu, Z., et al. (2019). Continental slope-confined canyons in the Pearl River Mouth basin in the South China sea dominated by erosion, 2004–2018. *Geomorphology*, 344, 60–74. <https://doi.org/10.1016/j.geomorph.2019.07.016>
- Liu, D., Li, X., Emeis, K.-C., Wang, Y., & Richard, P. (2015). Distribution and sources of organic matter in surface sediments of Bohai Sea near the Yellow River Estuary, China. *Estuarine, Coastal and Shelf Science*, 165, 128–136. <https://doi.org/10.1016/j.ecss.2015.09.007>
- Liu, J. P., Li, A. C., Xu, K. H., Velozzi, D. M., Yang, Z. S., Milliman, J. D., & DeMaster, D. J. (2006). Sedimentary features of the Yangtze River-derived along-shelf clinoform deposit in the East China Sea. *Continental Shelf Research*, 26(17–18), 2141–2156. <https://doi.org/10.1016/j.csr.2006.07.013>
- Liu, J. P., Xu, K. H., Li, A. C., Milliman, J. D., Velozzi, D. M., Xiao, S. B., & Yang, Z. S. (2007). Flux and fate of Yangtze River sediment delivered to the East China Sea. *Geomorphology*, 85(3–4), 208–224. <https://doi.org/10.1016/j.geomorph.2006.03.023>
- Liu, J. T., Hsu, R. T., Hung, J.-J., Chang, Y.-P., Wang, Y.-H., Rendle-Bühning, R. H., et al. (2016). From the highest to the deepest: The Gaoping River–Gaoping submarine canyon dispersal system. *Earth-Science Reviews*, 153, 274–300. <https://doi.org/10.1016/j.earscirev.2015.10.012>
- Liu, J. T., Hung, J.-J., Lin, H.-L., Huh, C.-A., Lee, C.-L., Hsu, R. T., et al. (2009). From suspended particles to strata: The fate of terrestrial substances in the Gaoping (Kaoping) submarine canyon. *Journal of Marine Systems*, 76(4), 417–432. <https://doi.org/10.1016/j.jmarsys.2008.01.010>
- Liu, K., Xiao, X., Zhang, D., Ding, Y., Li, L., & Zhao, M. (2021). Quantitative estimates of organic carbon contributions to the river-estuary-marine system in the Jiaozhou Bay, China. *Ecological Indicators*, 129, 107929. <https://doi.org/10.1016/j.ecolind.2021.107929>
- Liu, S., Shi, X., Fang, X., Dou, Y., Liu, Y., & Wang, X. (2014). Spatial and temporal distributions of clay minerals in mud deposits on the inner shelf of the East China Sea: Implications for paleoenvironmental changes in the Holocene. *Quaternary International*, 349, 270–279. <https://doi.org/10.1016/j.quaint.2014.07.016>
- Liu, X., Tang, D., & Ge, C. (2020). Distribution and sources of organic carbon, nitrogen and their isotopic composition in surface sediments from the southern Yellow Sea, China. *Marine Pollution Bulletin*, 150, 110716. <https://doi.org/10.1016/j.marpolbul.2019.110716>
- Liu, Z., Colin, C., Li, X., Zhao, Y., Tuo, S., Chen, Z., et al. (2010). Clay mineral distribution in surface sediments of the northeastern South China Sea and surrounding fluvial drainage basins: Source and transport. *Marine Geology*, 277(1–4), 48–60. <https://doi.org/10.1016/j.margeo.2010.08.010>
- Liu, Z., Zhao, Y., Colin, C., Statterger, K., Wiesner, M. G., Huh, C.-A., et al. (2016). Source-to-sink transport processes of fluvial sediments in the South China Sea. *Earth-Science Reviews*, 153, 238–273. <https://doi.org/10.1016/j.earscirev.2015.08.005>
- Mayer, L. M. (1994). Surface area control of organic carbon accumulation in continental shelf sediments. *Geochimica et Cosmochimica Acta*, 58(4), 1271–1284. [https://doi.org/10.1016/0016-7037\(94\)90381-6](https://doi.org/10.1016/0016-7037(94)90381-6)
- Meksumpun, S., Meksumpun, C., Hoshika, A., Mishima, Y., & Tanimoto, T. (2005). Stable carbon and nitrogen isotope ratios of sediment in the gulf of Thailand: Evidence for understanding of marine environment. *Continental Shelf Research*, 25(15), 1905–1915. <https://doi.org/10.1016/j.csr.2005.04.009>
- Milliman, J. D., & Farnsworth, K. L. (2011). *River discharge to the coastal ocean*. Cambridge University Press. <https://doi.org/10.1017/CBO9780511781247>
- Mitchell, P. J., Spence, M. A., Aldridge, J., Kotilainen, A. T., & Dying, M. (2021). Sedimentation rates in the Baltic Sea: A machine learning approach. *Continental Shelf Research*, 214, 104325. <https://doi.org/10.1016/j.csr.2020.104325>
- Mollenhauer, G., Kienast, M., Lamy, F., Meggers, H., Schneider, R. R., Hayes, J. M., & Eglinton, T. I. (2005). An evaluation of 14 C age relationships between co-occurring foraminifera, alkenones, and total organic carbon in continental margin sediments. *Paleoceanography*, 20(1), n/a–n/a. <https://doi.org/10.1029/2004PA001103>
- Narman, L. (2020). *Carbon transfer in the western South China Sea: Biogeochemical perspectives on organic carbon pools in surface sediments, from source to burial*. Heriot-Watt University.

- Paradis, S., Nakajima, K., van der Voort, T., Geis, H., Blattmann, T., Bröder, L., & Eglinton, T. (2023). The Modern Ocean sediment archive and inventory of carbon (MOSAIC): Version 2.0. *Earth System Science Data*, *15*(9), 4105–4125. <https://doi.org/10.5194/essd-15-4105-2023>
- Park, Y., & Khim, B. (1992). Origin and dispersal of recent clay minerals in the Yellow Sea. *Marine Geology*, *104*(1–4), 205–213. [https://doi.org/10.1016/0025-3227\(92\)90095-Y](https://doi.org/10.1016/0025-3227(92)90095-Y)
- Parker, S., Chen, X.-G., Loh, P. S., He, S., Jin, A.-M., Zhao, J., et al. (2022). Oceanographic and human impacts on the compositions of sedimentary organic matter along the southern coast of Zhoushan. *Journal of Marine Systems*, *227*, 103681. <https://doi.org/10.1016/j.jmarsys.2021.103681>
- Pedregosa, F., Varoquaux, G., Gramfort, A., Michel, V., Thirion, B., Grisel, O., et al. (2011). Scikit-learn: Machine learning in Python. *Journal of Machine Learning Research*, *12*(Oct), 2825–2830. Retrieved from <http://jmlr.csail.mit.edu/papers/v12/pedregosa1a.html>
- Qin, Y., Zheng, B., Lei, K., Lin, T., Hu, L., & Guo, Z. (2011). Distribution and mass inventory of polycyclic aromatic hydrocarbons in the sediments of the south Bohai Sea, China. *Marine Pollution Bulletin*, *62*(2), 371–376. <https://doi.org/10.1016/j.marpolbul.2010.09.028>
- Restrepo, G. A., Wood, W. T., & Phrampus, B. J. (2020). Oceanic sediment accumulation rates predicted via machine learning algorithm: Towards sediment characterization on a global scale. *Geo-Marine Letters*, *40*(5), 755–763. <https://doi.org/10.1007/s00367-020-00669-1>
- Shi, X., Shen, S., Yi, H., Chen, Z., & Meng, Y. (2003). Modern sedimentary environments and dynamic depositional systems in the southern Yellow Sea. *Chinese Science Bulletin*, *48*(S1), 1–7. <https://doi.org/10.1007/BF02900933>
- Sparkes, R. B., Lin, I. T., Hovius, N., Galy, A., Liu, J. T., Xu, X., & Yang, R. (2015). Redistribution of multi-phase particulate organic carbon in a marine shelf and canyon system during an exceptional river flood: Effects of Typhoon Morakot on the Gaoping River–Canyon system. *Marine Geology*, *363*, 191–201. <https://doi.org/10.1016/j.margeo.2015.02.013>
- Srisuksawad, K., Porntepkasemsan, B., Nouchpramool, S., Yamkate, P., Carpenter, R., Peterson, M., & Hamilton, T. (1997). Radionuclide activities, geochemistry, and accumulation rates of sediments in the Gulf of Thailand. *Continental Shelf Research*, *17*(8), 925–965. [https://doi.org/10.1016/S0278-4343\(96\)00065-9](https://doi.org/10.1016/S0278-4343(96)00065-9)
- Stattegger, K. (2001). (Table 1) Carbon analysis of surface sediments off Vietnam and from Sunda shelf. PANGAEA. <https://doi.org/10.1594/PANGAEA.59937>
- Sun, X., Fan, D., Cheng, P., Hu, L., Sun, X., Guo, Z., & Yang, Z. (2021). Source, transport and fate of terrestrial organic carbon from Yangtze River during a large flood event: Insights from multiple-isotopes ($\delta^{13}C$, $\delta^{15}N$, $\Delta^{14}C$) and geochemical tracers. *Geochimica et Cosmochimica Acta*, *308*, 217–236. <https://doi.org/10.1016/j.gca.2021.06.004>
- Szczuciński, W., Jagodziński, R., Hanebuth, T. J. J., Stattegger, K., Wetzel, A., Mitreǵa, M., et al. (2013). Modern sedimentation and sediment dispersal pattern on the continental shelf off the Mekong River delta, South China Sea. *Global and Planetary Change*, *110*, 195–213. <https://doi.org/10.1016/j.gloplacha.2013.08.019>
- Tao, S., Eglinton, T. I., Montluçon, D. B., McIntyre, C., & Zhao, M. (2016). Diverse origins and pre-depositional histories of organic matter in contemporary Chinese marginal sea sediments. *Geochimica et Cosmochimica Acta*, *191*, 70–88. <https://doi.org/10.1016/j.gca.2016.07.019>
- Tao, S., Eglinton, T. I., Zhang, L., Yi, Z., Montluçon, D. B., McIntyre, C., et al. (2018). Temporal variability in composition and fluxes of Yellow River particulate organic matter. *Limnology & Oceanography*, *63*(S1), S119–S141. <https://doi.org/10.1002/lno.10727>
- Tao, S., Liu, J. T., Wang, A., Blattmann, T. M., Yang, R. J., Lee, J., et al. (2022). Deciphering organic matter distribution by source-specific biomarkers in the shallow Taiwan Strait from a source-to-sink perspective. *Frontiers in Marine Science*, *9*. <https://doi.org/10.3389/fmars.2022.969461>
- Unverricht, D., Szczuciński, W., Stattegger, K., Jagodziński, R., Le, X. T., & Kwong, L. L. W. (2013). Modern sedimentation and morphology of the subaqueous Mekong delta, southern Vietnam. *Global and Planetary Change*, *110*, 223–235. <https://doi.org/10.1016/j.gloplacha.2012.12.009>
- van den Bergh, G. D., Boer, W., Schaapveld, M. A. S., Duc, D. M., & van Weering, T. C. E. (2007). Recent sedimentation and sediment accumulation rates of the Ba Lat prodelta (Red River, Vietnam). *Journal of Asian Earth Sciences*, *29*(4), 545–557. <https://doi.org/10.1016/j.jseas.2006.03.006>
- van der Voort, T. S., Blattmann, T. M., Usman, M., Montluçon, D., Loeffler, T., Tavagna, M. L., et al. (2021). MOSAIC (Modern Ocean sediment archive and inventory of carbon): A (radio)carbon-centric database for seafloor surficial sediments. *Earth System Science Data*, *13*(5), 2135–2146. <https://doi.org/10.5194/essd-13-2135-2021>
- Van der Voort, T. S., Mannu, U., Blattmann, T. M., Bao, R., Zhao, M., & Eglinton, T. I. (2018). Deconvolving the fate of carbon in coastal sediments. *Geophysical Research Letters*, *45*(9), 4134–4142. <https://doi.org/10.1029/2018GL077009>
- Vonk, J. E., Sánchez-García, L., van Dongen, B. E., Alling, V., Kosmach, D., Charkin, A., et al. (2012). Activation of old carbon by erosion of coastal and subsea permafrost in Arctic Siberia. *Nature*, *489*(7414), 137–140. <https://doi.org/10.1038/nature11392>
- Wang, C., Zhang, C., Wang, Y., Jia, G., Wang, Y., Zhu, C., et al. (2022). Anthropogenic perturbations to the fate of terrestrial organic matter in a river-dominated marginal sea. *Geochimica et Cosmochimica Acta*, *333*, 242–262. <https://doi.org/10.1016/j.gca.2022.07.012>
- Wang, F., Wang, H., Li, J., Pei, Y., Fan, C., Tian, L., et al. (2008). ^{210}Pb and ^{137}Cs measurements in the Circum Bohai Sea Coastal region: Sedimentation rates and implications. *Frontiers of Earth Science in China*, *2*(3), 276–282. <https://doi.org/10.1007/s11707-008-0046-5>
- Wang, X., & Li, A. (2007). Preservation of black carbon in the shelf sediments of the East China Sea. *Chinese Science Bulletin*, *52*(22), 3155–3161. <https://doi.org/10.1007/s11434-007-0452-1>
- Wang, X., Ma, H., Li, R., Song, Z., & Wu, J. (2012). Seasonal fluxes and source variation of organic carbon transported by two major Chinese Rivers: The Yellow River and Changjiang (Yangtze) River. *Global Biogeochemical Cycles*, *26*(2). <https://doi.org/10.1029/2011GB004130>
- Wei, B., Mollenhauer, G., Heftler, J., Grotheer, H., & Jia, G. (2020). Dispersal and aging of terrigenous organic matter in the Pearl River estuary and the northern South China Sea shelf. *Geochimica et Cosmochimica Acta*, *282*, 324–339. <https://doi.org/10.1016/j.gca.2020.04.032>
- Wei, L., Cai, P., Shi, X., Cai, W.-J., Liu, W., Hong, Q., et al. (2022). Winter mixing accelerates decomposition of sedimentary organic carbon in seasonally hypoxic coastal seas. *Geochimica et Cosmochimica Acta*, *317*, 457–471. <https://doi.org/10.1016/j.gca.2021.11.003>
- Wessel, P., & Smith, W. H. F. (1996). A global, self-consistent, hierarchical, high-resolution shoreline database. *Journal of Geophysical Research*, *101*(B4), 8741–8743. <https://doi.org/10.1029/96JB00104>
- Wiesner, M. G., Wetzel, A., Catane, S. G., Listanco, E. L., & Mirabueno, H. T. (2004). Grain size, areal thickness distribution and controls on sedimentation of the 1991 Mount Pinatubo tephra layer in the South China Sea. *Bulletin of Volcanology*, *66*(3), 226–242. <https://doi.org/10.1007/s00445-003-0306-x>
- Wu, B., Wu, X., Shi, X., Qiao, S., Liu, S., Hu, L., et al. (2020). Influences of tropical monsoon climatology on the delivery and dispersal of organic carbon over the Upper Gulf of Thailand. *Marine Geology*, *426*, 106209. <https://doi.org/10.1016/j.margeo.2020.106209>
- Wu, Y., Eglinton, T., Yang, L., Deng, B., Montluçon, D., & Zhang, J. (2013). Spatial variability in the abundance, composition, and age of organic matter in surficial sediments of the East China Sea. *Journal of Geophysical Research: Biogeosciences*, *118*(4), 1495–1507. <https://doi.org/10.1002/2013JG002286>

- Xing, L., Zhang, H., Yuan, Z., Sun, Y., & Zhao, M. (2011). Terrestrial and marine biomarker estimates of organic matter sources and distributions in surface sediments from the East China Sea shelf. *Continental Shelf Research*, 31(10), 1106–1115. <https://doi.org/10.1016/j.csr.2011.04.003>
- Xing, L., Zhao, M., Gao, W., Wang, F., Zhang, H., Li, L., et al. (2014). Multiple proxy estimates of source and spatial variation in organic matter in surface sediments from the southern Yellow Sea. *Organic Geochemistry*, 76, 72–81. <https://doi.org/10.1016/j.orggeochem.2014.07.005>
- Xu, K., Milliman, J. D., Li, A., Paul Liu, J., Kao, S.-J., & Wan, S. (2009). Yangtze- and Taiwan-derived sediments on the inner shelf of East China Sea. *Continental Shelf Research*, 29(18), 2240–2256. <https://doi.org/10.1016/j.csr.2009.08.017>
- Xue, Z., Paul Liu, J., DeMaster, D., Leithold, E. L., Wan, S., Ge, Q., et al. (2014). Sedimentary processes on the Mekong subaqueous delta: Clay mineral and geochemical analysis. *Journal of Asian Earth Sciences*, 79, 520–528. <https://doi.org/10.1016/j.jseas.2012.07.012>
- Yang, Q., Qu, K., Yang, S., Sun, Y., Zhang, Y., & Zhou, M. (2021). Environmental factors affecting regional differences and decadal variations in the buried flux of marine organic carbon in eastern shelf sea areas of China. *Acta Oceanologica Sinica*, 40(6), 26–34. <https://doi.org/10.1007/s13131-020-1601-5>
- Yang, Z., Ji, Y., Bi, N., Lei, K., & Wang, H. (2011). Sediment transport off the Huanghe (Yellow River) delta and in the adjacent Bohai Sea in winter and seasonal comparison. *Estuarine, Coastal and Shelf Science*, 93(3), 173–181. <https://doi.org/10.1016/j.ecss.2010.06.005>
- Yang, Z., Wang, H., Saito, Y., Milliman, J. D., Xu, K., Qiao, S., & Shi, G. (2006). Dam impacts on the Changjiang (Yangtze) river sediment discharge to the sea: The past 55 years and after the three Gorges Dam. *Water Resources Research*, 42(4). <https://doi.org/10.1029/2005WR003970>
- Yao, P., Yu, Z., Bianchi, T. S., Guo, Z., Zhao, M., Knappy, C. S., et al. (2015). A multiproxy analysis of sedimentary organic carbon in the Changjiang Estuary and adjacent shelf. *Journal of Geophysical Research: Biogeosciences*, 120(7), 1407–1429. <https://doi.org/10.1002/2014JG002831>
- Yao, P., Zhao, B., Bianchi, T. S., Guo, Z., Zhao, M., Li, D., et al. (2014). Remineralization of sedimentary organic carbon in mud deposits of the Changjiang Estuary and adjacent shelf: Implications for carbon preservation and authigenic mineral formation. *Continental Shelf Research*, 91, 1–11. <https://doi.org/10.1016/j.csr.2014.08.010>
- Yin, S., Lin, L., Pope, E. L., Li, J., Ding, W., Wu, Z., et al. (2019). Continental slope-confined canyons in the Pearl River Mouth Basin in the South China Sea dominated by erosion, 2004–2018. *Geomorphology*, 344, 60–74. <https://doi.org/10.1016/j.geomorph.2019.07.016>
- Yoon, S.-H., Kim, J.-H., Yi, H.-I., Yamamoto, M., Gal, J.-K., Kang, S., & Shin, K.-H. (2016). Source, composition and reactivity of sedimentary organic carbon in the river-dominated marginal seas: A study of the eastern Yellow Sea (the northwestern Pacific). *Continental Shelf Research*, 125, 114–126. <https://doi.org/10.1016/j.csr.2016.07.010>
- Yu, F., Zong, Y., Lloyd, J. M., Huang, G., Leng, M. J., Kendrick, C., et al. (2010). Bulk organic $\delta^{13}C$ and C/N as indicators for sediment sources in the Pearl River delta and estuary, southern China. *Estuarine, Coastal and Shelf Science*, 87(4), 618–630. <https://doi.org/10.1016/j.ecss.2010.02.018>
- Yu, M., Eglinton, T. I., Haghypour, N., Dubois, N., Wacker, L., Zhang, H., et al. (2022). Persistently high efficiencies of terrestrial organic carbon burial in Chinese marginal sea sediments over the last 200 years. *Chemical Geology*, 606, 120999. <https://doi.org/10.1016/j.chemgeo.2022.120999>
- Yu, M., Eglinton, T. I., Haghypour, N., Montluçon, D. B., Wacker, L., Hou, P., et al. (2019). Impacts of natural and human-induced hydrological variability on particulate organic carbon dynamics in the Yellow River. *Environmental Science & Technology*, 53(3), 1119–1129. <https://doi.org/10.1021/acs.est.8b04705>
- Yu, M., Eglinton, T. I., Haghypour, N., Montluçon, D. B., Wacker, L., Hou, P., et al. (2021). Contrasting fates of terrestrial organic carbon pools in marginal sea sediments. *Geochimica et Cosmochimica Acta*, 309, 16–30. <https://doi.org/10.1016/j.gca.2021.06.018>
- Zhang, Y., Kaiser, K., Li, L., Zhang, D., Ran, Y., & Benner, R. (2014). Sources, distributions, and early diagenesis of sedimentary organic matter in the Pearl River region of the South China Sea. *Marine Chemistry*, 158, 39–48. <https://doi.org/10.1016/j.marchem.2013.11.003>
- Zhang, Y., Xiao, X., Liu, D., Wang, E., Liu, K., Ding, Y., et al. (2020). Spatial and seasonal variations of organic carbon distributions in typical intertidal sediments of China. *Organic Geochemistry*, 142, 103993. <https://doi.org/10.1016/j.orggeochem.2020.103993>
- Zhao, B., Yao, P., Bianchi, T. S., Arellano, A. R., Wang, X., Yang, J., et al. (2018). The remineralization of sedimentary organic carbon in different sedimentary regimes of the Yellow and East China Seas. *Chemical Geology*, 495, 104–117. <https://doi.org/10.1016/j.chemgeo.2018.08.012>
- Zhao, B., Yao, P., Bianchi, T. S., & Yu, Z. G. (2021). Controls on organic carbon burial in the eastern China marginal seas: A regional synthesis. *Global Biogeochemical Cycles*, 35(4), e2020GB006608. <https://doi.org/10.1029/2020GB006608>
- Zhou, L., Liu, J., Saito, Y., Zhang, Z., Chu, H., & Hu, G. (2014). Coastal erosion as a major sediment supplier to continental shelves: Example from the abandoned old Huanghe (Yellow River) delta. *Continental Shelf Research*, 82, 43–59. <https://doi.org/10.1016/j.csr.2014.03.015>
- Zhu, C., Wagner, T., Pan, J.-M., & Pancost, R. D. (2011). Multiple sources and extensive degradation of terrestrial sedimentary organic matter across an energetic, wide continental shelf. *Geochemistry, Geophysics, Geosystems*, 12(8), Q08011. <https://doi.org/10.1029/2011GC003506>
- Zhu, C., Wang, Z.-H., Xue, B., Yu, P.-S., Pan, J.-M., Wagner, T., & Pancost, R. D. (2011). Characterizing the depositional settings for sedimentary organic matter distributions in the lower Yangtze River-East China Sea shelf system. *Estuarine, Coastal and Shelf Science*, 93(3), 182–191. <https://doi.org/10.1016/j.ecss.2010.08.001>
- Zhu, Y., & Chang, R. (2000). Preliminary study of the dynamic origin of the distribution pattern of bottom sediments on the continental shelves of the Bohai Sea, Yellow Sea and East China Sea. *Estuarine, Coastal and Shelf Science*, 51(5), 663–680. <https://doi.org/10.1006/ecss.2000.0696>